Received: 31 October 2020 | Revised: 22 December 2020 | Accepted: 22 December 2020

DOI: 10.1111/mmi.14676

RESEARCH ARTICLE

WILEY

The PfAP2-G2 transcription factor is a critical regulator of gametocyte maturation

Suprita Singh [1,2] | Joana M. Santos [1,2] | Lindsey M. Orchard [1,2] | Naomi Yamada [4] | Riëtte van Biljon [1,2,4] | Heather J. Painter [1,2] | Shaun Mahony [1,4] | Manuel Llinás [1,2,3,4]

[1]Department of Biochemistry and Molecular Biology, The Pennsylvania State University, University Park, PA, USA

[2]Huck Center for Malaria Research, The Pennsylvania State University, University Park, PA, USA

[3]Department of Chemistry, The Pennsylvania State University, University Park, PA, USA

[4]Center for Eukaryotic Gene Regulation, Department of Biochemistry & Molecular Biology, The Pennsylvania State University, University Park, PA, USA

Correspondence
Manuel Llinás, Department of Biochemistry and Molecular Biology, The Pennsylvania State University, University Park, PA 16802, USA.

Present address
Joana M. Santos, Institute for Integrative Biology of the Cell (I2BC), CEA, CNRS, Université Paris-Saclay, Gif-sur-Yvette, 91198, France
Naomi Yamada, GSK R&D Functional Genomics, 1250 S. Collegeville Rd., Collegeville, PA 19426, USA
Heather J. Painter, Division of Bacterial, Parasitic, and Allergenic Products, Office of Vaccines Research and Review, U.S. Food and Drug Administration, Center for Biologics Evaluation and Research, 10903 New Hampshire Ave, Silver Spring, MD 20993, USA

Funding information
National Institute of Allergy and Infectious Diseases, Grant/Award Number: 1R01 AI125565

Abstract

Differentiation from asexual blood stages to mature sexual gametocytes is required for the transmission of malaria parasites. Here, we report that the ApiAP2 transcription factor, PfAP2-G2 (PF3D7_1408200) plays a critical role in the maturation of *Plasmodium falciparum* gametocytes. PfAP2-G2 binds to the promoters of a wide array of genes that are expressed at many stages of the parasite life cycle. Interestingly, we also find binding of PfAP2-G2 within the gene body of almost 3,000 genes, which strongly correlates with the location of H3K36me3 and several other histone modifications as well as Heterochromatin Protein 1 (HP1), suggesting that occupancy of PfAP2-G2 in gene bodies may serve as an alternative regulatory mechanism. Disruption of *pfap2-g2* does not impact asexual development, but the majority of sexual parasites are unable to mature beyond stage III gametocytes. The absence of *pfap2-g2* leads to overexpression of 28% of the genes bound by PfAP2-G2 and none of the PfAP2-G2 bound genes are downregulated, suggesting that it is a repressor. We also find that PfAP2-G2 interacts with chromatin remodeling proteins, a microrchidia (MORC) protein, and another ApiAP2 protein (PF3D7_1139300). Overall our data demonstrate that PfAP2-G2 establishes an essential gametocyte maturation program in association with other chromatin-related proteins.

KEYWORDS

ApiAP2, gametocyte, malaria, PfAP2-G2, *Plasmodium falciparum*

1 | INTRODUCTION

Malaria is a life-threatening disease that continues to impact the lives of millions of people worldwide. According to the latest WHO estimates, there were 228 million cases of malaria in 2018, resulting in 405,000 deaths (World Malaria Report, WHO, 2019). Malaria is caused by unicellular protozoan parasites belonging to the genus *Plasmodium*. Of the six species that infect humans, *Plasmodium falciparum* has the highest mortality rate (Weiss et al., 2019; WHO, 2019). *P. falciparum* exhibits a complex life cycle with asexual and sexual erythrocytic phases in the human host, followed by development in *Anopheles* mosquitoes which transmit the parasite back to a new host, initiating the pre-erythrocytic liver stage of infection. Although the cyclic 48-hr asexual blood-stage is responsible for symptomatic disease and severe malaria, this form of the parasite cannot be transmitted. Rather, in each round of replication, a fraction of the parasites (<10%) exit the asexual pathway and undergo sexual differentiation to form male and female gametocytes, which are transmission competent (Bruce et al., 1989). Inhibition of gametocyte development is of great interest, because it would prevent malaria parasite transmission, which is one of the major goals in the effort to achieve disease eradication (Rabinovich et al., 2017).

Gametocyte development in *P. falciparum* is a 9–12 day process, which is substantially longer than that of other human infecting *Plasmodium* species such as *P. vivax* and the rodent malaria parasites *P. berghei* (26–30 hr) and *P. yoelii* (36 hr) (Armistead et al., 2018; Gautret & Motard, 1999; Liu et al., 2011). *P. falciparum* gametocyte development is divided into five (stage I to V) morphologically distinct stages (Sinden, 1982). The earliest phase of gametocyte development, stage Ia, occurs around 24 to 30 hr post-invasion (hpi) and is morphologically indistinguishable from the young trophozoite stage. However, there are several well-defined markers of early stage I gametocytes such as Pfs16, Pfg27, and PfGEXP-5 (Alano et al., 1991; Bruce et al., 1994; Josling et al., 2020; Llorà-Batlle et al., 2020; Poran et al., 2017; Silvestrini et al., 2010). In the human host, stage Ib to stage IV sexually developing parasites are sequestered in deep tissues like the bone marrow and only stage V gametocytes freely circulate in the blood and can be picked up by mosquitoes (Aguilar et al., 2014; Joice et al., 2014; Venugopal et al., 2020).

Regulation of *Plasmodium* development is driven by stage-specific transcription factors (TFs), such as the well-studied Apicomplexan AP2 (ApiAP2) family of DNA-binding proteins. ApiAP2 proteins are found among all members of the phylum, and each ApiAP2 protein contains between one and three Apetala2 (AP2) DNA binding domains (Balaji et al., 2005; Painter et al., 2011). In *P. falciparum* there are 27 members of the ApiAP2 protein family. ApiAP2 proteins have been shown to control all developmental transitions in *Plasmodium* (Jeninga et al., 2019; Modrzynska et al., 2017; Zhang et al., 2017).

A master regulator of sexual (gametocyte) commitment, AP2-G, has been identified in both *P. falciparum* and *Plasmodium berghei*, a rodent malaria parasite (Kafsack et al., 2014; Sinha et al., 2014). Expression levels of PfAP2-G (PF3D7_1222600) strongly correlate with the formation of gametocytes, and targeted disruption of the *pfap2-g* locus results in a complete block in gametocytogenesis and downregulation of many gametocyte-associated genes (Kafsack et al., 2014). Another regulator of *Plasmodium* gametocyte development is AP2-G3. Disruption of *pyap2-g3* (PY17X_1417400) in *P. yoelii* resulted in significant reduction in the numbers of male and female gametocytes, day 8 oocysts, and sporozoites, but it did not affect the asexual growth of the parasites (Zhang et al., 2017). The *P. berghei* orthologue, PBANKA_1415700, has also been disrupted and shown to be female specific and essential for female gametocyte development, and was thus renamed PbAP2-FG (Yuda et al., 2020). The *P. falciparum* orthologue, PF3D7_1317200, was also found to be associated with gametocytogenesis (Ikadai et al., 2013), although it has not been extensively characterized.

AP2-G2 has been shown to play a role in gametocytogenesis in both *P. berghei* and *P. yoelii* (Modrzynska et al., 2017; Sinha et al., 2014; Yuda et al., 2015). Deletion of *pbap2-g2* does not inhibit sexual stage conversion but rather results in the nearly complete loss of gametocyte maturation and a block in transmission to mosquitoes (Yuda et al., 2015). Yuda et al. reported that this *P. berghei* transcription factor is bound to roughly 1,500 genes, or slightly over 1/3 of the genome during asexual development, and a number of these genes were upregulated by more than two-fold in *pbap2-g2* knockout lines. In another study, disruption of *pbap2-g2* also caused premature expression of liver stage and sporozoite stage genes during asexual development in red blood cells (Modrzynska et al., 2017). Moreover, a *P. berghei* liver-stage (LS) transcriptome of *P. berghei* reported strong upregulation of *pbap2-g2* in early LS that is negatively correlated with the expression of liver stage-specific transcripts (Toro-Moreno et al., 2020). Together, these findings suggest that AP2-G2 acts as a repressor in both the asexual and sexual stages and during early liver-stage infection in *P. berghei*. Accordingly, *P. yoelii* parasites lacking the *pyap2-g2* gene had greatly reduced numbers of gametocytes and oocysts (Zhang et al., 2017). A recent genome-wide knockout screen suggests that AP2-G2 is also not essential for blood-stage development in *P. falciparum* (Zhang et al., 2018), and may have a role in a later stage of development.

In this study we explore the function of AP2-G2 in *P. falciparum* during parasite blood-stage development. The period of gametocyte maturation for rodent malaria parasites is shorter than in *P. falciparum*, making it difficult to discern the developmental phenotypes associated with *ap2-g2* knockouts. Therefore, disrupting this gene in *P. falciparum* is of interest due to the longer maturation period. Furthermore, two studies have reported differences in asexual blood-stage development resulting from *pbap2-g2* deletion. On one hand, Modrzynska *et al*. observed reduced growth and premature expression of liver- and sporozoite-stage genes (Modrzynska et al., 2017). Conversely, Yuda et al. reported that *pbap2-g2*- parasites proliferate normally in blood (Yuda et al., 2015). Another discrepancy regards the impact of the gene deletion on the sex ratio. Sinha *et al*. reported a difference in the ratio of male to female gametocytes in *pbap2-g2*- lines (Sinha et al., 2014) while Yuda et al. observed no such differences (Yuda et al., 2015).

We find that the *P. falciparum orthologue* of AP2-G2 also plays a critical role in the maturation of gametocytes. Disruption of *pfap2-g2* does not impact asexual development, parasite multiplication rate, or

commitment to sexual development, but most parasites are unable to develop normally beyond stage III gametocytes. Using transcriptomic analysis and ChIP-seq we have identified a number of candidate genes that are bound and regulated by PfAP2-G2. We also identify interacting partners using protein immunoprecipitation followed by mass spectrometry. Overall our work suggests that PfAP2-G2 is a transcriptional repressor that likely recruits additional transcription factors and chromatin remodeling machinery to the genome to control gene expression. PfAP2-G2 plays a critical role in the regulation of the development of malaria parasites as they transition from asexual to sexual parasites, allowing for proper gametocyte maturation.

2 | RESULTS

2.1 | PfAP2-G2 is expressed during the trophozoite and schizont stages of asexual development

The *P. falciparum* orthologue of AP2-G2, PF3D7_1408200, encodes a 189kDa protein that contains a single AP2 DNA-binding domain (Figure 1a). *pfap2-g2* is maximally transcribed at the ring and early trophozoite stages (Bozdech et al., 2003; Painter et al., 2018) and proteomics data indicate protein expression occurs at the trophozoite and schizont stages (Oehring et al., 2012). To precisely determine the timing of PfAP2-G2 expression and its subcellular localization, we tagged the gene at the C-terminus with GFP (Figure S1a). Using live-cell fluorescence microscopy, we imaged a highly synchronized PfAP2-G2::GFP parasite population for one complete asexual replication cycle, every 7 hr beginning with the newly invaded ring stage (2–5 hpi) revealed that PfAP2-G2 was localized to the nucleus, as expected, and was expressed from the early trophozoite to the late schizont stages (Figure 1b). Further confirming the nuclear localization of PfAP2-G2, nuclear fractionation of trophozoite stage parasites (~30 hpi) showed that full length PfAP2-G2::GFP (~250 kDa) was only detected in the nuclear fraction of the parasite lysates (Figure 1c). We also detected other smaller sized peptides indicating that PfAP2-G2 may be degraded during the preparation of parasite lysate or is proteolytically cleaved. No bands were detected in a WT 3D7 control (Figure S1b).

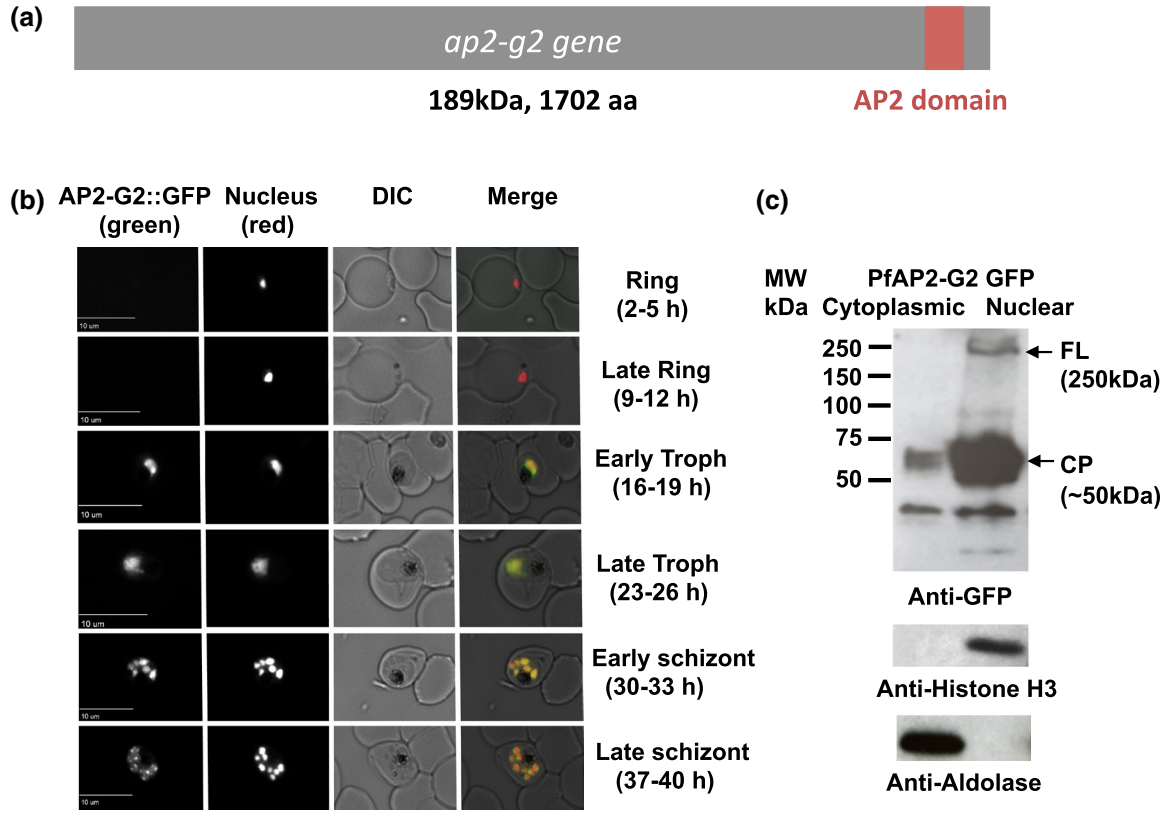

FIGURE 1 PfAP2-G2 is expressed from around 16–19 hpi in asexual stage parasites (a) Structure of the PfAP2-G2 protein which contains a single AP2 DNA-binding domain. (b) Live fluorescence microscopy performed on a highly synchronized population of AP2-G2::GFP parasites every 7 hr of the asexual life cycle showed that PfAP2-G2::GFP colocalizes with the nucleus in both the trophozoite and schizont stages. DRAQ-5 was used as the nuclear stain. (c) Nuclear and cytoplasmic fractions from synchronized trophozoite stage parasites expressing GFP-tagged PfAP2-G2 were subjected to western blot analysis using anti-GFP antibodies (1:1,000). Full-length (FL) GFP-tagged PfAP2-G2 (~250 kDa) was detected only in the nuclear fraction of the parasite lysate whereas a cleavage product (CP, ~50kDa) was found in both fractions. Anti-histone H3 (1:3,000) and anti-aldolase (1:1,000) were used as fractionation controls for the nuclear and cytoplasmic fractions, respectively. WT parasites were used as a negative control (Figure S1b).

2.2 | PfAP2-G2 is not required for proliferation during the asexual stages of the life cycle

To determine the role *of pfap2-g2*, we generated a genetic disruption (KO) line using selection linked integration (SLI) (Birnbaum et al., 2017) to truncate the *pfap2-g2* coding sequence and isolated several clones (Figure S2a). As expected, *pfap2-g2* KO parasites were readily obtained. Live-cell fluorescence imaging of the transgenic parasites showed diffuse cytoplasmic staining, suggesting that the remaining non AP2 domain-containing protein fragment is localised largely outside the nucleus (Figure S2b). We next determined if truncation of PfAP2-G2 impacted asexual stage parasite growth or multiplication rate. Using a SYBR green growth assay (Vossen et al., 2010), we find that *pfap2-g2* KO parasites develop similarly to WT (Figure 2a), and have similar multiplication rates (Figure 2b). Therefore, although PfAP2-G2 is expressed in the asexual blood stages, it is not required for normal asexual development.

2.3 | PfAP2-G2 is expressed in the gametocyte stages

Recent transcriptomic data have shown that the mRNA abundance of *pfap2-g2* in gametocytes is low relative to the asexual stages, with a broad peak seen only in the early gametocyte stages followed by low expression during the later stages (Figure S3) (Van Biljon et al., 2019). To characterize protein expression of PfAP2-G2 during gametocyte development we imaged PfAP2-G2::GFP parasites (see methods). PfAP2-G2 was expressed in all stages of gametocyte development, but it was not confined to the nucleus in later stages (Figure 3a). Indeed, nuclear fractionation of stage III gametocytes detected expression of full-length protein in both fractions, unlike in asexual parasites (Figure 3b). It also seems that the nuclear protein may undergoe different proteolytic processing in gametocytes versus the asexual stages.

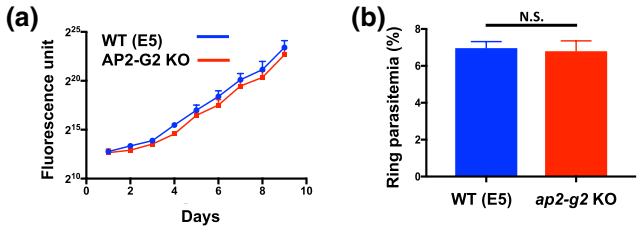

FIGURE 2 Absence of PfAP2-G2 has no effect on the growth of asexual blood stage parasite (a) Growth profiles of the WT and *pfap2-g2* KO parasites measured using an SYBR green assay every 24 hr over a period of 10 days starting with highly synchronous ring-stage parasites. The graph represents the plotted average ± S.D. of biological triplicates. Fluorescence units are plotted along the Y-axis and the number of days was plotted along the X-axis (ANOVA $p = .65$). (b) Measurement of the ring parasitemia (multiplication rate) of the WT and *pfap2-g2* KO parasites. The values are the average of three biological replicates, and the error bars represent the standard deviation ($p = .5$, not significant [N.S.])

2.4 | PfAP2-G2 is essential for gametocyte maturation

To determine if sexually committed *pfap2-g2* KO gametocytes mature fully to stage V, we induced PfAP2-G2 WT and KO parasite lines to undergo gametocytogenesis and followed their development for 14 days, monitoring their maturation via morphological analysis of Giemsa-stained thin-blood smears. Whereas WT parasites matured into stage V gametocytes by Day 9–11, most *pfap2-g2* KO parasites committed to sexual development did not progress beyond stage III (Figure 3c). We also noticed that a larger proportion of dead or morphologically abnormal gametocytes were present in the *pfap2-g2* KO compared to the WT in later time points, and only 2% of the *pfap2-g2* KO resembled mature stage V gametocytes at Day 11, compared to 30% in the parental line (Figure 3c). PfAP2-G2 is, thus, a critical regulator of gametocyte maturation and development.

2.5 | PfAP2-G2 makes extensive genome-wide interactions

Because PfAP2-G2 is predicted to be a DNA-binding protein (Campbell et al., 2010; Yuda et al., 2015) we sought to determine the genome-wide localization of PfAP2-G2 in both asexual and gametocyte life cycle stages. To do this we first performed ChIP-seq at the trophozoite stage using the PfAP2-G2::GFP parasites. Peak calling identified ~5,000 peaks in at least two of the three biological replicates (FDR 0.05) (Figure S4a). All replicates showed a high correlation with each other with respect to the overall peaks identified (Figure 4a). To our surprise only 401 of the predicted binding sites, corresponding to 94 genes, were found in the upstream non-coding regions of genes (Table S1), while 4,600 peaks, corresponding to 2,932 genes, were located in exonic gene bodies (Table S2). This differs from what has been previously observed for other characterized *P. falciparum* ApiAP2 proteins, such as SIP2 (Flueck et al., 2010), AP2-I (Santos et al., 2017) and AP2-G (Josling et al., 2020), which were found to predominantly bind to non-coding 5' upstream regions. Although wide-scale binding to gene bodies was not previously reported for PbAP2-G2 (Yuda et al., 2015), a re-analysis of the ChIP-seq data from that study using the same pipeline that we used for our ChIP-seq data analysis, revealed that PbAP2-G2 is also broadly distributed across gene bodies in the *P. berghei* genome with 4,345 binding sites (Table S3).

An analysis of all the regions (both upstream regions and ORFs) bound by PfAP2-G2, using DREME (Bailey, 2011) identified two significantly enriched DNA sequence motifs. The first is an AGAA sequence motif related to a previously reported DNA motif found to associate with one (of the three) AP2 domains of the ApiAP2 protein PF3D7_1139300 (Campbell et al., 2010). The second is an ACCA

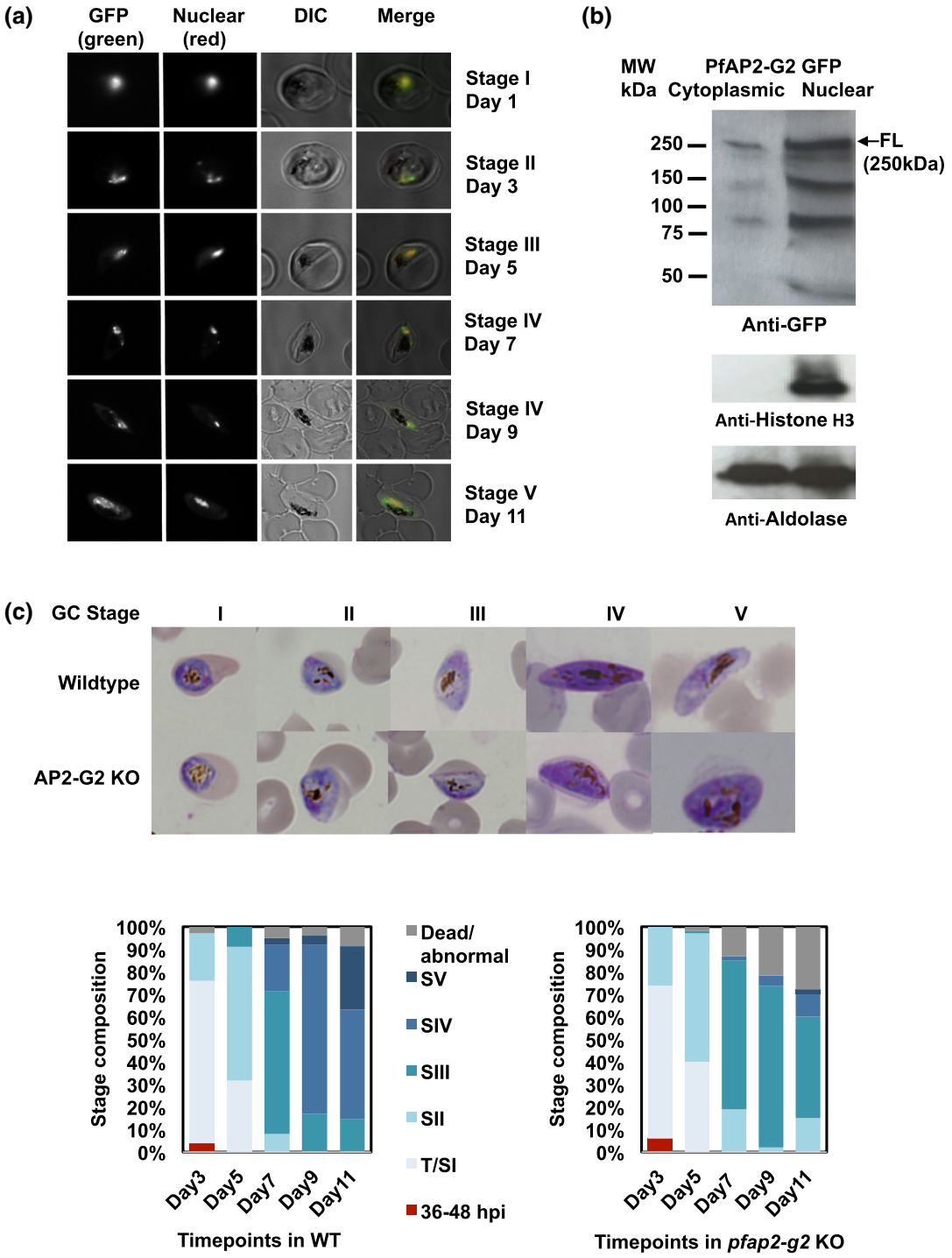

FIGURE 3 PfAP2-G2 is expressed throughout the gametocyte stages and is essential for maturation of gametocytes (a) Images obtained by live fluorescence microscopy performed on Stage I through Stage V gametocytes. The DIC image was merged with the DRAQ5 nuclear stain imaging to confirm the nuclear localization of the signal. The results indicate that PfAP2-G2 was expressed at all stages of gametocyte development and was localized to the nucleus. (b) Nuclear and cytoplasmic fractions from stage III gametocytes were subjected to western blot analysis using anti-GFP antibodies (1:1,000). The GFP-tagged AP2-G2 of expected size (~250 kDa) was detected in both the nuclear and cytoplasmic fractions of the parasite lysate. Anti-histone H3 (1:3,000) and anti-aldolase (1:1,000) were used as the loading controls for the nuclear and cytosolic fractions, respectively. (c) Giemsa-stained smears of gametocytes from the WT and PfAP2-G2 KO lines showed that the morphology of the KO gametocytes appeared normal until Stage III. Most *pfap2-g2* KO parasites committed to sexual development did not progress beyond stage III. Morphological staging was quantified by counting ≥ 100 parasites for each time point during gametocyte development from Giemsa-stained smears. The reported number of counts are based on a single replicate.

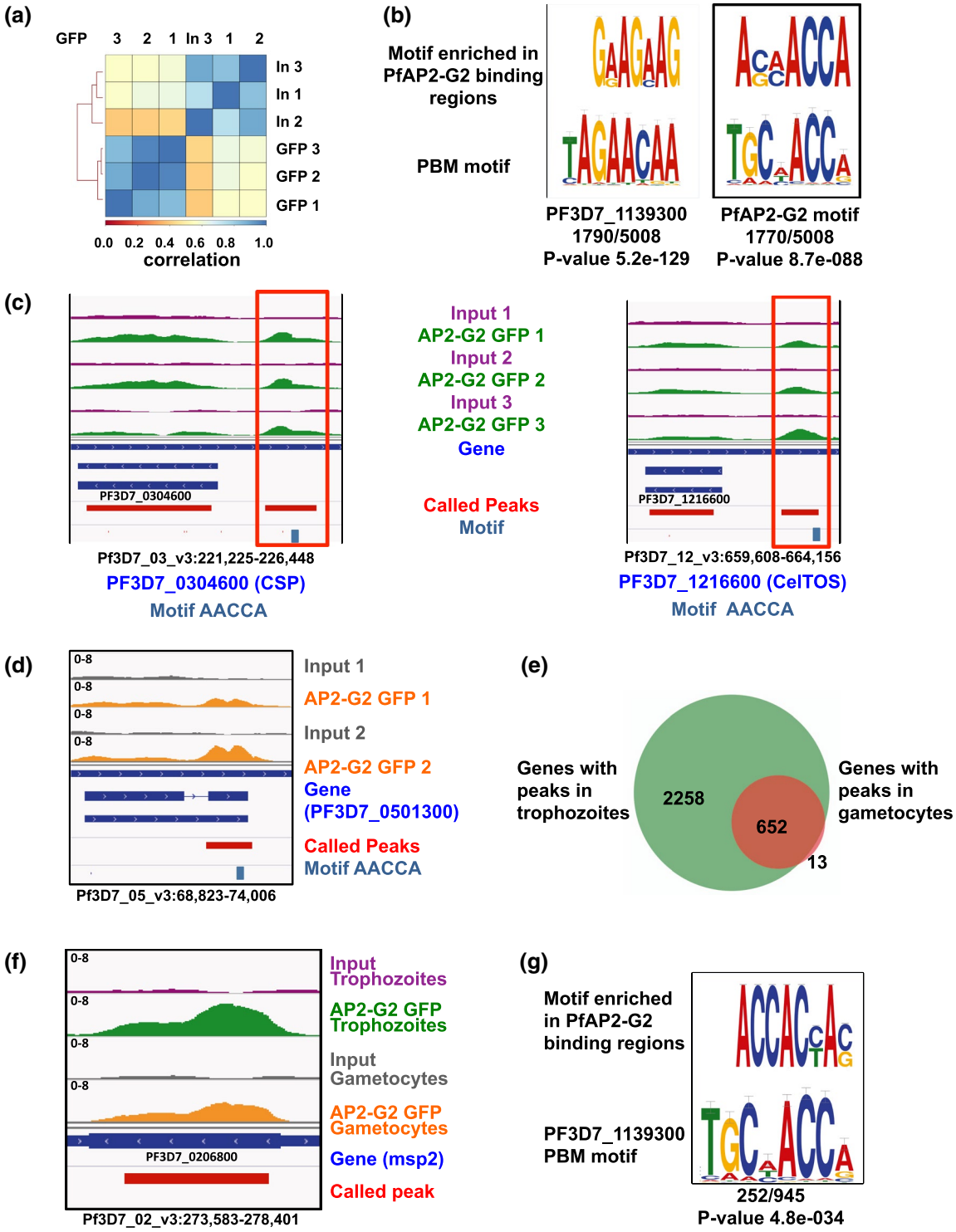

FIGURE 4 Genome-wide predictions of PfAP2-G2 targets and binding regions by ChIP-seq (a) Pearson correlation analysis of three biological replicates of ChIP-seq including the Input (In) and AP2-G2 GFP (GFP) (b) DREME logos for the motifs enriched in the genomic locations bound by PfAP2-G2 in the gene bodies and non-coding regions in the asexual stage. Shown is the enriched PF3D7_1139300 motif AGAA and PfAP2-G2 motif ACCA obtained by DREME along with the PBM motif. The P-values reported are generated by DREME. (c) Example of PfAP2-G2 peaks in asexual stages for all three ChIP-seq replicates. Peaks are represented as red tracks below with the DNA motifs highlighted in blue. (d) Example of PfAP2-G2 peaks in gametocytes for both replicates. (e) Venn diagram showing genes with PfAP2-G2 peaks in both trophozoite and gametocyte stages. (f) Representative peaks for PfAP2-G2 binding upstream of the *msp2* gene in both trophozoite and gametocyte stages. (g) DREME logo for the motifs enriched in the genomic locations bound by PfAP2-G2 in the gene bodies and non-coding regions in gametocytes. The P-values reported are generated by DREME.

core motif (Figure 4b), which closely resembles the previously identified PfAP2-G2 target motif obtained by protein binding microarrays (PBM) (Campbell et al., 2010).

In order to characterize possible regulatory targets of PfAP2-G2, we first focused on the 94 genes that contained PfAP2-G2 peaks in their upstream regions. Nearly 87% of these 94 putative target genes are bound within 2.5 kb upstream of the start codon (Figure S4b). 278 of the remaining intergenic peaks were localized to the subtelomeric ends of each chromosome (Figure S4c). For further analysis we only considered genes with upstream binding interactions less than 2.5 kb from the start codon, leaving 82 candidate genes (Table S1). Interestingly, PfAP2-G2 at the asexual trophozoite stage binds to the promoters of genes known to be expressed later in the gametocyte and mosquito life cycle stages. These include 6-cysteine protein (*p36* PF3D7_0404400), cysteine repeat modular protein 2 (*crmp2* PF3D7_0718300), sporozoite protein essential for cell traversal (*spect* PF3D7_1342500), circumsporozoite protein (*csp* PF3D7_0304600), cell traversal protein for ookinetes and sporozoites (*celtos* PF3D7_1216600), secreted protein altered thrombospondin repeat protein (*spatr* PF3D7_0212600), stearoyl-CoA desaturase (*scd* PF3D7_0511200), and *cap380* oocyst capsule protein (PF3D7_0320400) among others (Table S1) (Chattopadhyay et al., 2003; van Dijk et al., 2010; Espinosa et al., 2017; Gratraud et al., 2009; Ishino et al., 2004; Itsara et al., 2018; Singh et al., 2007; Thompson et al., 2007; Zhao et al., 2016). Representative PfAP2-G2 peaks upstream of two target genes are shown in (Figure 4c). We also found that PfAP2-G2 associated with the upstream regions of genes that are highly transcribed in the asexual ring stage (as analyzed in López-Barragán et al., 2011) including the knob-associated histidine rich protein (*kahrp* PF3D7_0202000), *Plasmodium* helical interspersed subtelomeric proteins (*phista* PF3D7_0115100), several variant family genes including *vars* and *rifins* and genes encoding proteins involved in egress and invasion such as the Rh5 interacting protein (*ripr* PF3D7_0323400) and serine repeat antigen 7 (*sera7* PF3D7_0207400) (Miller et al., 2002; Pei et al., 2005; Sargeant et al., 2006; Volz et al., 2016). Therefore, PfAP2-G2 binds to the promoters and ORFs of genes that are expressed at a different developmental stage than that in which *pfap2-g2* is expressed. This suggests that, as in the rodent malaria species, PfAP2-G2 is a transcriptional repressor protein that prevents the premature expression of later stage genes.

Since the developmental arrest we observed in *pfap2-g2* KO parasites occurred at state III gametocytes, we next examined the genome-wide occupancy of PfAP2-G2 in stage III gametocytes by ChIP-seq. We identified 947 peaks in common across two replicates, corresponding to 674 genes at an FDR of 0.05 (Figure 4d) (Tables S4 and S5). PfAP2-G2 binding, once again, was found in both upstream regions and within gene bodies. Although PfAP2-G2 bound many fewer regions in gametocytes compared to trophozoites, which may be associated with the difficulty in obtaining high amounts of chromatin in gametocytes, virtually all stage III PfAP2-G2 target genes were also targets during the trophozoite stages (Figure 4e). This suggests that there are a large number of genes that are always bound by PfAP2-G2 during both asexual and sexual parasite development (Figure 4f). DNA motif analysis yet again identified the ACCA motif as being bound by PfAP2-G2 in gametocytes (Figure 4g).

2.6 | Genetic disruption of PfAP2-G2 leads to aberrant gene expression in both asexual and sexual stages

Using synchronized parasites, we collected seven total RNA samples from WT or KO parasites throughout the 48 hr asexual life cycle for transcriptome analysis (parasite counts are in (Figure S5). In a separate experiment, total RNA samples were collected during sexual differentiation every 12 hr for 7 continuous days starting at 2 days post-gametocyte induction (Figure S6a,b). Gene expression analysis of the asexual blood stage time course using Significance Analysis of Microarray (SAM) (Tusher et al., 2001) identified 327 differentially expressed transcripts (>1.5 log2FC, 0.30 local FDR) in the *pfap2-g2* KO line. Out of these, 237 showed enhanced transcript abundance in the *pfap2-g2* KO line and 90 showed decreased abundance (Figure S7, Table S6). This result is quite surprising given the lack of any asexual growth phenotype between the *pfap2-g2* KO and the WT (Figure 2), implying that these changes in gene expression do not impact asexual parasite fitness or gametocyte commitment. A comparison of transcript abundance in the KO and WT sexual stages identified increased abundance for 274 transcripts and reduced abundance for 169 transcripts in the *pfap2-g2* KO line (>1.5 log2FC, 0.30 local FDR) (Figure S7, Table S7). These differential transcription patterns presumably lead to the stall in development at Stage III gametocytes in parasites lacking PfAP2-G2.

To determine at which stage the significantly differential mRNAs (by SAM) are maximally transcribed in wild-type parasites, we used a published RNA-seq dataset covering four different asexual blood stages (rings, early trophozoite, late trophozoite, and schizonts), two gametocyte stages (stage II and stage V), and the ookinete stage using the 3D7 *P. falciparum* strain (López-Barragán et al., 2011). Using this dataset, we identified the 3D7 parasite lifecycle stage at which each gene has the highest fragments per kilobase of transcript, per million mapped sequencing reads (FPKM). For the asexual transcriptome, most of the differentially expressed genes we measured as differentially regulated in the *pfap2-g2* KO are normally transcribed maximally in stage V gametocyte (and not in asexual stages), followed by the ookinete and ring stages (Figure 5a). This suggests that loss of PfAP2-G2 impacts the expression of genes from late-stage gametocytes, ookinetes, and asexual stages. However, the number of genes showing enhanced transcript abundance is strikingly high for genes that are normally expressed in stage V gametocytes (Figure 5a). Therefore, PfAP2-G2 may prevent the premature expression of late-stage gametocyte genes during asexual development.

In the gametocyte transcriptome, we observed the opposite trend when comparing to the López-Barragán data, where 70% of the transcripts that showed increased abundance in the KO line were maximally abundant in the asexual stages, especially at the ring stage

(Figure 5a). Examples of protein products whose mRNA transcript abundance was higher in gametocytes include the knob-associated histidine-rich protein (KAHRP, PF3D7_0202000), 15 *Plasmodium* helical interspersed subtelomeric proteins (PHISTs), 7 members of the FIKK serine/threonine protein kinase family proteins, 12 Plasmodium exported hypothetical gene family proteins (HYPs), the merozoite surface proteins MSP1, MSP2, MSP6, MSP7, MSP9, and MSP11, the ApiAP2 transcription factor AP2-L (PF3D7_0730300),

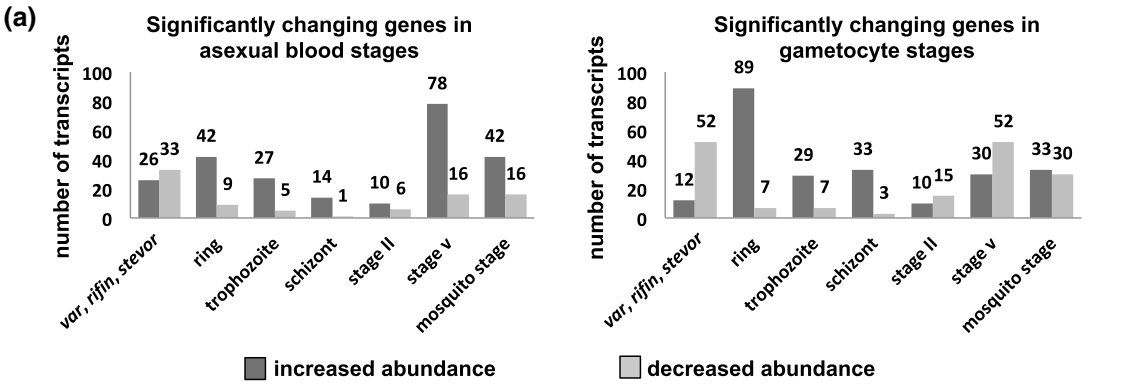

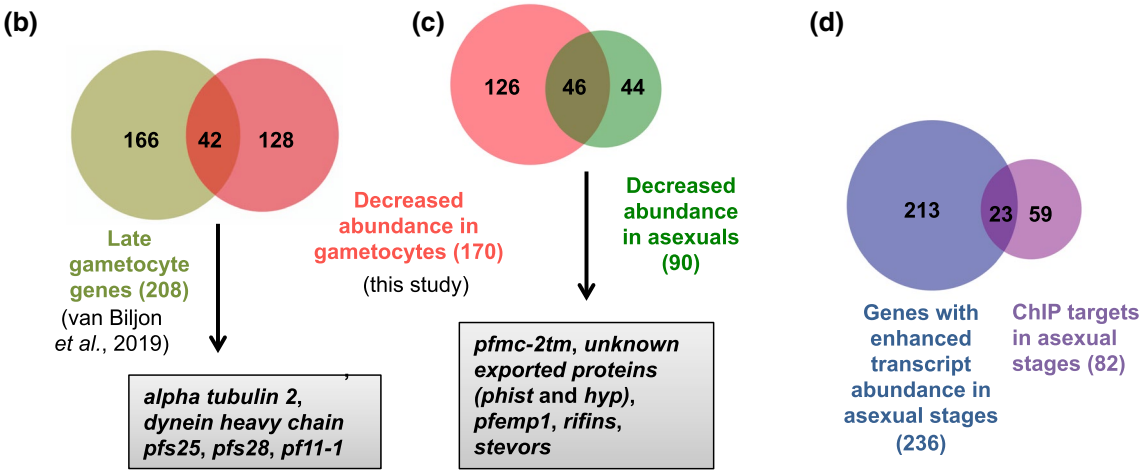

(e)

PF3D7_0212600	secreted protein with altered thrombospondin repeat domain
PF3D7_0207400	serine repeat antigen 7
PF3D7_0216800	TMEM121 domain-containing protein, putative
PF3D7_0202000	knob-associated histidine-rich protein
PF3D7_0200100	erythrocyte membrane protein 1, PfEMP1
PF3D7_0323400	Rh5 interacting protein
PF3D7_0320400	oocyst capsule protein Cap380
PF3D7_0304600	circumsporozoite (CS) protein
PF3D7_0301800	Plasmodium exported protein, unknown function
PF3D7_0511200	stearoyl-CoA desaturase
PF3D7_0632800	erythrocyte membrane protein 1, PfEMP1
PF3D7_0702100	Plasmodium exported protein (PHISTb), unknown function, pseudogene
PF3D7_0800100	erythrocyte membrane protein 1, PfEMP1
PF3D7_0931300	conserved Plasmodium protein, unknown function
PF3D7_0936100	early transcribed membrane protein
PF3D7_1016500	Plasmodium exported protein (PHISTc), unknown function
PF3D7_1102000	DnaJ protein, putative
PF3D7_1100100	erythrocyte membrane protein 1, PfEMP1
PF3D7_1252900	Plasmodium exported protein, unknown function
PF3D7_1327100	conserved protein, unknown function
PF3D7_1447500	inner membrane complex protein, putative
PF3D7_1455600	ferlin, putative
PF3D7_1477800	acyl-CoA binding protein

(f)

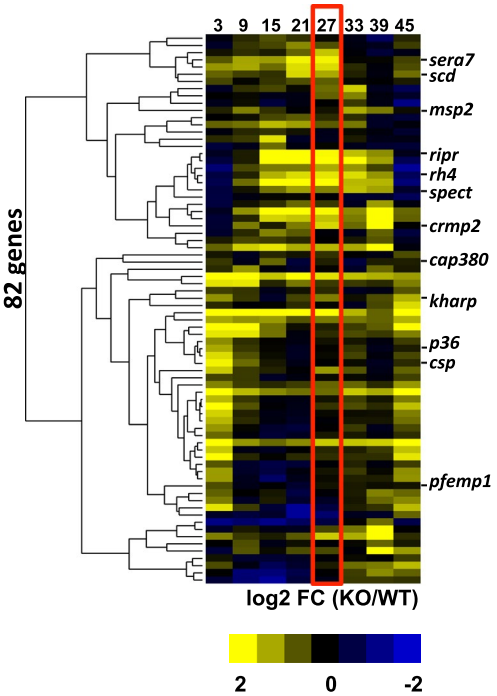

FIGURE 5 Transcriptional changes in parasites lacking PfAP2-G2 (a) Classification of significantly changing genes in asexual and gametocyte stages based on their maximum transcription in either asexual, gametocyte or mosquito stages, using RNA-seq data (López-Barragán et al., 2011). (b) Overlap between the genes with decreased transcript abundance in gametocytes and established late gametocyte markers (Figure 2, cluster 9 from Van Biljon et al., 2019). (c) Overlap between genes with decreased transcript abundance in gametocytes and asexual stages. (d) Overlap of genes with PfAP2-G2 enrichment in the upstream regions and increased transcript abundance in the *pfap2-g2* KO (analyzed by SAM, >1.5 log2FC, 0.30 local FDR). (e) List of genes with PfAP2-G2 enrichment in the upstream regions and increased transcript abundance in the *pfap2-g2* KO (f) Expression fold change (log2 KO versus WT) for genes bound by PfAP2-G2 in the upstream regions during the asexual blood stages. The genes are clustered based on Pearson's correlation. Boxed is the time point at which ChIP-seq was performed

and serine repeat antigen 5 (SERA5, PF3D7_0207600) among others (Table S7) (Beeson et al., 2016; Nunes et al., 2007; Pei et al., 2005; Sargeant et al., 2006). These results indicate that PfAP2-G2 represses a subset of genes throughout both asexual and sexual development, and the absence of PfAP2-G2 leads to aberrant timing of gene expression.

To identify enriched DNA sequence motifs associated with gene expression changes, we analyzed the 5' upstream region (1,000 bp upstream of the start codon) of the genes showing significant change in transcript abundance in the asexual and sexual stages using the Finding Informative Regulatory Elements (FIRE) algorithm (Elemento et al., 2007). The most significant enriched sequence motif was the known DNA-interacting motif for PfAP2-G2, TGCAACCA (P-value 1.24 e-21) in genes with enhanced transcript abundance in the asexual stage (Figure S7). Interestingly, we also found an AGAACAA (P-value 3.36 e-15) DNA-binding motif that is recognized by the ApiAP2 protein, PF3D7_1139300 (Figure S7). Similar motifs were found for genes with increased transcript abundance in gametocytes (Figure S7). Intriguingly both *pfap2-g2* and *pf3d7_1139300* (*pf11_0404*) are expressed at similar times throughout asexual development based on transcriptomic data, suggesting that the two proteins may be acting together in some manner to regulate transcription (Figure S8). Based on earlier evidence, genetic disruption of the *pf3d7_1139300* orthologue in *P. berghei* (*pbanka_0909600*) and *P. yoelii* (*py17x_0911000*) was refractory, indicating its essentiality (Modrzynska et al., 2017; Zhang et al., 2017). Single-cell RNA-seq has shown a sharp upregulation of the gene encoding the ApiAP2 protein PF3D7_1139300 when *ap2-g* expression peaks just before egress in committed schizonts (Poran et al., 2017). Although we couldn't detect the ACCA PfAP2-G2 binding motif associated with genes showing decreased transcript abundance (Figure S9), we found enrichment of the AGACA motif, which has been associated with gametocyte commitment and development (Figure S9) (Bischoff & Vaquero, 2010; Painter et al., 2017; Young et al., 2005), in genes showing decreased transcript abundance in gametocytes.

Genes with decreased mRNA abundance in the gametocyte transcriptome from the *pfap2-g2* KO line (170 genes) overlap significantly with genes previously reported as late gametocyte markers (Van Biljon et al., 2019) (Figure 5b). Some example genes are alpha tubulin 2 (PF3D7_0422300), TRAP-like protein (*tlp* PF3D7_0616500), secreted ookinete protein (*psop13* PF3D7_0518800, *psop20* PF3D7_0715400), dynein heavy chain (PF3D7_0729900), ookinete surface protein P28 (PF3D7_1031000), and ookinete surface protein P25 (PF3D7_1031000) (Duffy & Kaslow, 1997; Ecker et al., 2008; Heiss et al., 2008; Rawlings et al., 1992; Villard et al., 2007). Therefore, one reason that *pfap2-g2* KO parasites may fail to progress beyond stage III may be due to the aberrant expression of mRNAs required during this and subsequent stages of gametocyte development. The inhibition of gametocyte maturation may also be due to the decreased expression of a few critical genes required for gametocyte development, such as male development gene 1 (*mdv1*, PF3D7_1216500), gametocyte erythrocyte cytosolic protein (*geco*, PF3D7_1253000), gametocyte exported protein (*gexp06* PF3D7_0114000), and gametocyte specific protein (*pf11-1*, PF3D7_1038400) during the asexual stage. Interestingly, we also see overlap between the genes with decreased transcript abundance in both the asexual and gametocyte stages. These overlapping genes are enriched mostly for members of the *var*, *stevor*, and *rifin* variant gene families, *Pfmc-2tm* among others (Figure 5c). An early gametocyte proteome revealed that exported and erythrocyte remodeling proteins are the most overrepresented proteins in gametocytes (Silvestrini et al., 2010). Although members of the PfEMP1, STEVOR and RIFIN protein repertoire are expressed in gametocyte stages, their role is not well established (Mwakalinga et al., 2012; Neveu & Lavazec, 2019; Neveu et al., 2018; Petter et al., 2008; Sharp et al., 2006; Tibúrcio et al., 2012, 2013), and decreased abundance of these genes may contribute to the observed phenotypic effect.

2.7 | PfAP2-G2 binding in the promoter and in gene bodies is associated with differential regulation of transcription

Out of 82 genes with upstream PfAP2-G2 peaks at the trophozoite stage, only 23 displayed significantly elevated mRNA abundance in the *pfap2-g2* KO (as analyzed by SAM, >1.5 log2FC, 0.30 local FDR) (Figure 5d,e). This suggests that the transcription of other genes may be impacted indirectly in the PfAP2-G2 knockout. On the other hand, none of the genes with significantly reduced mRNA abundance were bound by PfAP2-G2 in the upstream regions. However, considering the stage at which ChIP was performed we see that the mRNA abundance of many of the PfAP2-G2 ChIP-seq targets do not change in the absence of PfAP2-G2, indicating that binding of PfAP2-G2 alone might not be sufficient to affect transcription (Figure 5f). PfAP2-G2 binding to gene bodies results in both repression and activation of gene expression in the *pfap2-g2* KO. Open reading frames bound by PfAP2-G2 in the gene body in gametocytes showed similar effects

(Figure S10). Overall these results indicate that PfAP2-G2 binding to the upstream promoter region is largely associated with repression, but PfAP2-G2 alone is not sufficient to repress transcription.

2.8 | PfAP2-G2 shares occupancy with exonic epigenetic marks during asexual development

To understand the role of the pervasive genome-wide PfAP2-G2 binding in exonic gene bodies detected by ChIP-seq (Table S2), we investigated whether PfAP2-G2 is associated with any known epigenetic marks. We calculated a pairwise Pearson correlation coefficient by comparing the read counts per 1,000 bp bins of the PfAP2-G2 ChIP-seq results against an array of histone marks for which ChIP data are available: H3K9me3, H4ac, H4K20me3, H3K26ac, H3K9ac, H3K4me3 (Karmodiya et al., 2015), H3K36me2, and H3K36me3 (Jiang et al., 2013), as well as heterochromatin protein 1 (PfHP1) (Brancucci et al., 2014). Interestingly, we found that PfAP2-G2 occupancy has the strongest correlation with H3K36me3 (R = 0.933), followed by H4K20me3 (R = 0.911), H3K27ac (R = 0.826), and H4ac (R = 0.765) (Figure 6a), which are all histone marks that show moderate positive correlation with *P. falciparum* transcription and are associated with transcriptionally poised genes (Karmodiya et al., 2015). In total, 3,633 (80%) PfAP2-G2 binding sites co-occur with H3K36me3 marks (Figure 6b,c). The functional role of this association between PfAP2-G2 and H3K36me3 and what the potential role of PfAP2-G2 in H3K36me3 recruitment remain to be determined.

2.9 | PfAP2-G2 interacts with the chromatin remodeling machinery

To identify proteins potentially interacting in a complex with PfAP2-G2, we performed immunoprecipitations (IP) from

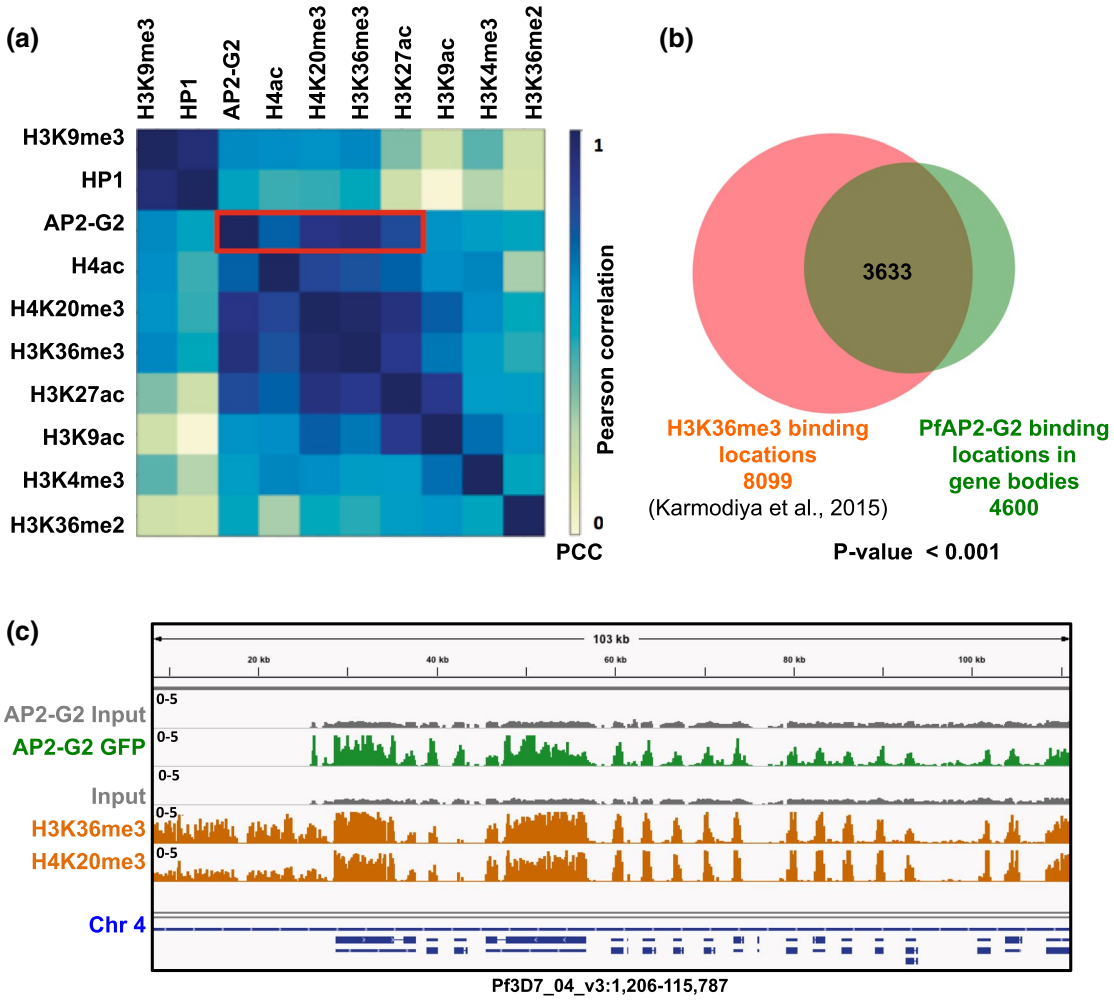

FIGURE 6 PfAP2-G2 shows high correlation with repressive histone modifications (a) Heatmap showing correlation between occupancy of PfAP2-G2 and nine histone modifications in the gene body of all *P. falciparum* genes (n = 5,735). PfAP2-G2 strongly correlates with H3K36me3 and H4K20me3 (b) Overlap of the peaks obtained by ChIP-seq on H3K36me3 marks (orange) (Jiang et al., 2013) and PfAP2-G2-GFP (green) shows 80% co-occupancy between PfAP2-G2 and H3K36me3 modified histones. (c) IGV screenshot showing co-occupancy of PfAP2-G2 with H3K36me3 and H4K20me3. First gray track represents the input for PfAP2-G2 and the second green track shows the regions bound by PfAP2-G2. The third gray track represents input for H3K36me3 and H4K20me3 and the last two orange tracks represent the regions bound by H3K36me3 and H4K20me3 as indicated in the figure. Blue track shows genes in this region

PfAP2-G2::GFP parasites at the trophozoite stage without crosslinking using an anti-GFP antibody. Western blot analysis confirmed that the full length PfAP2-G2 protein was purified and eluted (Figure 7a), although smaller GFP-positive band(s) were prevalent. The resulting IP was separated by SDS PAGE and two regions of the gel (upper and lower band, Figure 7a) were subjected to protein analysis by mass spectrometry. The purpose of analyzing these bands separately was to ensure that we could detect all of the proteins including the low abundance protein which otherwise would be masked when analyzing all of the bands together (Figure 7b).

The proteomic IP data were analyzed using SAINT (Choi et al., 2011) with a pSAINT score of 0.9 or higher and 1% FDR across all three replicates (Table S8). Although several high abundance cytoplasmic proteins (HSP70, RPS15) were detected, the majority are known to be localized to the nucleus. Reassuringly, both the upper and lower bands contained the PfAP2-G2 DNA–binding domain fused to GFP (Figure 7b). In the lower band we also identified histone protein 1 (HP1), the FACT complex proteins (FACT-S and FACT-L), and several histones (Figure 7c). The upper band contained larger chromatin remodeling proteins such as ISWI, SNF2L, GCN5, FACT-L, SPT5, and a MORC family protein (Figure 7d). We also found an association with two other ApiAP2 family proteins, including PF3D7_1139300 (PF11_0404) whose motif was found to be enriched in both the transcription and ChIP-seq data, suggesting that this interaction may be required for the regulation of a subset of target genes. Overall, these results demonstrate that PfAP2-G2

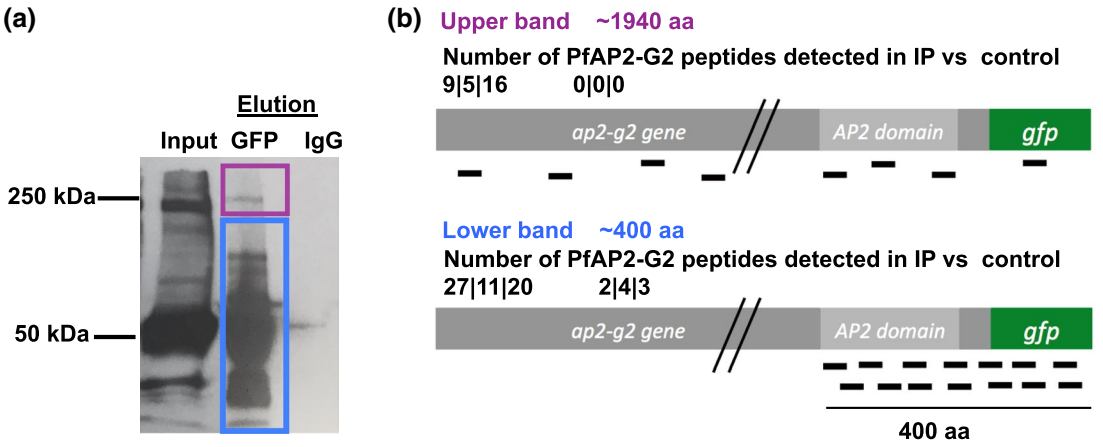

(c) **PfAP2-G2 interacting partners in the lower band**

Gene ID	Gene Description	Peptides in replicate IPs	Peptides in control	Average Probability
PF3D7_1408200	transcription factor with AP2 domain(s) (AP2-G2)	27|11|20	2|4|3	N/A
PF3D7_1105100	histone H2B (H2B)	24|11|14	0|2|1	1
PF3D7_1441400	FACT complex subunit SSRP1, putative (FACT-S)	17|11|11	0|2|2	1
PF3D7_0617900	histone H3 variant, putative (H3.3)	16|8|9	0|0|0	1
PF3D7_0917900	heat shock protein 70 (HSP70)	13|8|12	0|0|0	1
PF3D7_0517400	FACT complex subunit SPT16, putative (FACT-L)	19|8|12	0|0|0	1
PF3D7_1358800	40S ribosomal protein S15 (RPS15)	5|5|5	0|0|0	0.9997
PF3D7_1105000	histone H4 (H4)	37|14|22	0|3|6	0.9993
PF3D7_1220900	heterochromatin protein 1 (HP1)	13|5|6	0|1|0	0.999

FIGURE 7 (Continued)

(d) **PfAP2-G2 interacting partners in the upper band**

Gene ID	Gene Description	Peptides in replicate IPs	Peptides in control	Average Probability
PF3D7_1408200	transcription factor with AP2 domain(s) (AP2-G2)	9|5|16	0|0|0	N/A
PF3D7_0624600	SNF2 helicase, putative (ISWI)	28|14|27	0|1|5	1
PF3D7_1212700	eukaryotic translation initiation factor 3 subunit A, putative (EIF3A)	13|17|22	0|0|1	1
PF3D7_0607000	translation initiation factor IF-2, putative	11|5|14	0|0|0	1
PF3D7_0711000	AAA family ATPase, CDC48 subfamily (Cdc48)	7|10|10	0|2|0	0.9997
PF3D7_0710200	conserved Plasmodium protein, unknown function	6|6|23	0|0|0	0.9997
PF3D7_1104200	chromatin remodeling protein (SNF2L)	15|7|12	0|3|0	0.9993
PF3D7_1007700	transcription factor with AP2 domain(s) (ApiAP2)	13|6|6	0|0|1	0.9993
PF3D7_0517400	FACT complex subunit SPT16, putative (FACT-L)	7|4|8	0|0|0	0.999
PF3D7_1468100	MORC family protein, putative	14|8|17	0|1|3	0.9983
PF3D7_1433500	DNA topoisomerase 2 (TOP2)	9|8|16	0|0|4	0.9983
PF3D7_1008100	conserved Plasmodium protein, unknown function	4|5|14	0|0|0	0.998
PF3D7_0823300	histone acetyltransferase GCN5 (GCN5)	5|5|8	0|1|0	0.998
PF3D7_0500800	mature parasite-infected erythrocyte surface antigen (MESA)	36|28|42	0|8|7	0.9977
PF3D7_0811200	ER membrane protein complex subunit 1, putative (EMC1)	5|3|7	0|0|0	0.9977
PF3D7_1462300	conserved Plasmodium protein, unknown function	4|7|12	0|0|0	0.9973
PF3D7_0610900	transcription elongation factor SPT5, putative (SPT5)	5|7|8	0|1|0	0.9957
PF3D7_1023900	chromodomain-helicase-DNA-binding protein 1 homolog, putative (CHD1)	30|12|33	0|3|4	0.9933
PF3D7_1139300	transcription factor with AP2 domain(s) (ApiAP2)	2|2|3	0|0|0	0.967

FIGURE 7 Identification of potential interacting partners of PfAP2-G2 (a) Western blot showing immunoprecipitation (without crosslinking) of the PfAP2-G2 GFP parasite line using antibodies against GFP. Full-length PfAP2-G2 and the lower molecular weight cleaved product were analyzed separately by mass spectrometry to identify interacting partners of PfAP2-G2. (b) Schematic showing the number and location of PfAP2-G2 peptides recovered from the upper and lower bands. (c) List of PfAP2-G2-associated proteins in the lower band with high probability of interaction measured by SAINT (pSAINT 0.9 and 1%FDR). (d) List of PfAP2-G2-associated proteins in the upper band with high probability of interaction measured by SAINT (pSAINT 0.9 and 1%FDR)

does not function alone, but rather interacts with a number of chromatin remodeling proteins as well as established transcription associated factors, although the presence of different complexes is likely.

3 | DISCUSSION

Gametocytogenesis in *P. falciparum* parasites is a long, 10–12 day developmental progression resulting in the formation of fertile male and female gametes that will form a zygote only upon transmission to the mosquito host. Recent studies have shed light on the commitment and differentiation of asexual parasites into sexual parasites, (reviewed in Rea et al., 2018 and Josling et al., 2018) which is driven by the AP2-G master regulator (Josling et al., 2020; Kafsack et al., 2014; Sinha et al., 2014). However, how asexual cells are reprogrammed for gametocyte commitment, and the downstream post-commitment regulation of sexual development is not well characterized. There are known examples of gametocyte stage genes such as *pfsegxp*, *mdv1*, *gexp02* and *pfs16* that are expressed very early on in the asexual stages, suggesting that programming for gametocytogenesis may begin early in asexual development, and disruption of this program could result in profound effects post-commitment during sexual development (Furuya et al., 2005; Joice et al., 2014; Nixon et al., 2018; Painter et al., 2017; Portugaliza et al., 2020).

In this study, we show that the ApiAP2 protein PfAP2-G2 is essential for the development and maturation of *P. falciparum* gametocytes. PfAP2-G2 is expressed from the very early trophozoite stage through to stage V gametocytes. This is in contrast to *P. berghei*, where the protein is expressed from 16hpi, during the schizont stage of development (Yuda et al., 2015). Live fluorescence microscopy

and nuclear fractionation show that PfAP2-G2 is localized to the nucleus of the trophozoite, schizont, and early gametocyte stages (Figure 1b). In later stage gametocytes PfAP2-G2 protein levels are reduced and expressed throughout the cytoplasm (Figure 3a). This is consistent with the mRNA abundance profile, demonstrating peak *pfap2-g2* expression in the early asexual stages, whereas in gametocytes its expression is broad and weak (Van Biljon et al., 2019). The nuclear localization and strength of protein expression indicate that PfAP2-G2 is functionally important during the asexual stages and in early gametocytes.

By performing genome-wide ChIP-seq analysis at the asexual trophozoite stage and stage III gametocytes, we show that PfAP2-G2 binds extensively to both intergenic and genic regions. We note that the ChIP-seq results likely arise from full-length PfAP2-G2::GFP as well as smaller protein fragments (Figures 1c, 3b and 7b) that also contain the C-terminal AP2-domain fused to GFP. Genes bound by PfAP2-G2 in the upstream regions are largely expressed later in the gametocyte and mosquito stages. However, PfAP2-G2 also binds the promoters of genes expressed in the asexual ring stage and genes that are transcribed in schizont stages like *msps* encoding the merozoite surface proteins, which are regulated by PfAP2-I (Santos et al., 2017). Of course MSPs are unlikely to be required in committed gametocytes, as they no longer egress from the red blood cell for subsequent re-invasion. Interestingly, genes bound by PfAP2-G2 in stage III gametocytes are essentially the same as those bound in trophozoites. An analysis of the DNA motifs enriched in the regions bound by PfAP2-G2 identified two motifs: an AGAA motif and an ACCA motif (Figure 4b,g). The latter resembles the PBM-based predicted motif for PfAP2-G2, but it is different from that identified in *P. berghei* (GTTGT), even though the AP2 DNA-binding domain is highly conserved (97% identical). We also found enrichment for a second motif in the PfAP2-G2-bound regions, which resembles the in vitro DNA sequence motif bound by the ApiAP2 protein PF3D7_1139300 (PF11_0404) (Campbell et al., 2010). Supporting the hypothesis that these ApiAP2 proteins may function together in a complex, our immunoprecipitation experiments against PfAP2-G2::GFP detected AP2 PF3D7_1139300 (PF11_0404) as an interaction partner (Figure 7d, Table S8).

Parasites expressing a truncated PfAP2-G2 (*pfap2-g2* KO) proliferate normally in the asexual blood stages. These results are surprising given the many global transcriptional (327 transcripts, >1.5 log2FC, 0.30 local FDR) changes occurring in the asexual stages, and suggests that the parasite is tolerant to large fluctuations in gene expression. Compared with wild-type parasites, the expression levels of 90 genes (>1.5 log2FC, 0.30 local FDR) were significantly decreased during asexual development in *pfap2-g2* KO parasites, including genes that have been reported to have functional roles in gametocytes, perhaps leading to the developmental stall observed in stage III gametocytes (Van Biljon et al., 2019; Painter et al., 2017). This suggests that the program for sexual progression is established very early, in the asexual stage. KO of PbAP2-G2 also resulted in the downregulation of gametocyte genes (Yuda et al., 2015). Genes upregulated in the *pfap2-g2* KO were mostly those normally expressed at other later developmental stages including the gametocyte and ookinete stages (Figure 5a). In the upstream promoter regions of genes showing increased transcript abundance in the *pfap2-g2* KO, we found an enrichment of the PfAP2-G2 ACCA motif. PfAP2-G2, therefore, is involved in the repression of a number of genes that are not required for asexual development.

A previous study that examined the genome-wide binding of AP2-G2 from *P. berghei* gametocytes using ChIP-seq reported PbAP2-G2 binding at over 1,500 genes that were mostly associated with roles in asexual-stage proliferation (Yuda et al., 2015). Transcriptome analysis in gametocytes revealed the upregulation of 927 genes by more than twofold in *pbap2-g2* KO lines, suggesting that PbAP2-G2 acts as a repressor for asexual-stage genes during sexual development. However, only 397 (26.5%) of the PbAP2-G2 bound genes were upregulated in the *pbap2-g2* KO, leading Yuda et al. to hypothesize that relieving repression was not sufficient for the upregulation of the rest of the genes. Similarly, in our *pfap2-g2* KO transcriptomic data, not all genes that are bound by PfAP2-G2 show enhanced transcript abundance; only 23/82 genes with upstream PfAP2-G2 peaks (28%) displayed significantly elevated mRNA abundance. In fact, the PfAP2-G2 motif is only present in the promoter of genes upregulated in both developmental stages indicating that, as in *P. berghei*, PfAP2-G2 occupancy is not always predictive of changes in gene expression, perhaps because it requires interaction with other proteins. None of the genes bound by PfAP2-G2 in the upstream region are downregulated in the *pfap2-g2* KO, again highlighting the repressive action of PfAP2-G2.

The effect of PfAP2-G2 truncation upon transcript abundance is more pronounced in gametocytes. Unfortunately, due to the massive dysregulation of mRNA transcripts, it is difficult to ascertain the specific genes that cause the stall in development observed at stage III gametocytes. The significantly upregulated genes in gametocytes are mostly thought to be important for asexual blood stage development, similar to what was shown in *P. berghei* (Yuda et al., 2015). Interestingly, the ApiAP2 protein AP2-L, which plays a critical role in liver-stage development, is upregulated in the gametocyte stage in both the *P. falciparum* and *P. berghei ap2-g2* knockouts, and parasites lacking PbAP2-G2 are unable to cause liver infection (Yuda et al., 2015).

We observed a moderate to strong correlation between PfAP2-G2 occupancy and that of H3K9me3 (R = 0.933), followed by H4K20me3 (R = 0.911), H3K27ac (R = 0.826), H4ac (R = 0.765) and PfHP1 (R = 0.6) (Figure 6a). H3K36 methylation is a well-studied histone modification in model organisms, and carries out several roles. Studies in metazoans have shown that H3K36me3 is enriched at gene exons and plays a role in the regulation of alternative splicing (Kolasinska-Zwierz et al., 2009). Although H3K36me3 correlates with active transcription, another study found an association of this modification with facultative heterochromatin (Chantalat et al., 2011). Thus, H3K36me3 is involved with both actively transcribed as well as silenced regions and may contribute

to the formation of heterochromatin in combination with other histone modifications. At a subset of heterochromatic genes, binding to HP1a is required for enzyme-mediated H3K36me3 demethylation, suggesting that there are different ways in which H3K36me3 regulates chromatin (Lin et al., 2012). In *P. falciparum*, H3K36me3 is present along the entire gene body of silent *var* genes including the transcription start site (TSS), and it is deposited by the *P. falciparum* variant-silencing methyltransferase containing a SET domain (PfSETvs) (Jiang et al., 2013). However, enrichment of H3K36me3 was also found at the 3' end of other ring-stage active genes besides the variable antigen *var*, *rifin*, and *stevor* genes in PfSET KO parasites. This result indicates there is an alternative methyltransferase associated with H3K36 methylation.

We also found that PfHP1 localized with PfAP2-G2 toward the end of the chromosomes and is associated with both sub-telomeric and chromosome-internal *var* genes and *Plasmodium*-exported proteins (Figure S11a,b). A direct interaction between PfHP1 and PfAP2-G2 was supported by IP-MS (Figure 7c). PfAP2-G2 also shows perinuclear localization as previously described for PfHP1 and repressed *var* genes (Figure S12) (Flueck et al., 2009; Guizetti et al., 2013). However, future experiments are needed to determine a direct functional link between PfAP2-G2 and HP1. We also found a significant association between PfAP2-G2 and the MORC protein PF3D7_1468100 (Figure 7d). MORC proteins have been identified to play important roles in chromatin compaction in plants and animals and was recently established as the upstream transcriptional repressor of sexual commitment in *Toxoplasma gondii* (Farhat et al., 2020). This study found that MORC forms a complex with *T. gondii* ApiAP2 transcription factors at sexual stage genes. Two of the *T. gondii* ApiAP2 proteins found to associate with MORC by IP-MS are TgAP2IV-2 and TgAP2IX-9, whose AP2 DNA-binding domains are most identical to the PfAP2-G2 AP2 domain (Farhat et al., 2020). PfAP2-G2 also interacts with the *P. falciparum* ISWI chromatin-remodeling protein (Figure 7d), which was recently identified in a complex with the MORC protein at *var* gene promoters (Bryant et al., 2020). We speculate that PfAP2-G2 plays a role in regulating regions of the genome which need to be silenced to prevent spurious transcription.

Previous studies have shown that expression of the master gametocyte regulator *pfap2-g* peaks at two distinct points during asexual blood stage development (Poran et al., 2017). The initial *pfap2-g* expression peak in trophozoites is associated with the activation of genes encoding ISWI, SNF2L, and the ApiAP2 protein P3D7_1222400. The second expression peak occurs just before merozoite egress from committed schizonts and leads to the expression of genes encoding LSD2, HDA1 and the AP2-G2 associated ApiAP2 protein PF3D7_1139300 (Poran et al., 2017). Therefore, we propose that PF3D7_1139300 may act in a complex with PfAP2-G2 to compress chromatin structure. In summary, we have demonstrated that PfAP2-G2 plays an important role in gene repression in concert with other chromatin-related proteins during the maturation of the *P. falciparum* parasite sexual stages.

4 | MATERIALS AND METHODS

4.1 | Construction of plasmids for tagging the 3'end of *pfap2-g2* for *pfap2-g2* gene disruption

The pDC2-cam-CRT-GFP (Fidock et al., 2000) plasmid was used to tag the 3' end of the gene *pfap2-g2* with *gfp*. A 948 bp homologous fragment from the 3' end of the gene was amplified from 3D7 genomic DNA using the oligonucleotide pairs (Forward Primer P7 and Reverse Primer P8, see primer list), which also encoded restriction sites BglII and XhoI for cloning. This fragment was ligated into the BglII-and XhoI-digested pDC2-cam-CRT-GFP resulting in the final vector pDC2-cam-AP2-G2-GFP.

To create the *pfap2-g2* disrupted line, the *ap2-g2* gene locus was targeted using the selection linked integration (SLI) method (Birnbaum et al., 2017). To do this a 500 bp fragment of the 5' end of *pfap2-g2* was amplified using a forward primer with a NotI restriction site as well as a single point mutation in the homologous sequence to introduce a stop codon (Forward Primer P9) and a reverse primer with an MluI site (Reverse Primer P10) to be ligated into the final vector. This fragment was cloned (in frame) into pSLI-TGD using NotI and MluI restriction sites resulting in the final vector, pSLI-TGD-AP2-G2. A list of all oligonucleotide primers used is available in Table S9.

4.2 | Culturing, synchronization, transfection, and cloning of *P. falciparum* parasites

Plasmodium falciparum parasites were cultured as previously described (Trager & Jensen, 2005) and maintained in 6% O_2 and 5% CO_2 and grown in sterile filtered RPMI 1640 media (Gibco) supplemented with 2 M HEPES, $NaHCO_3$ (2 g/L), 0.1 M hypoxanthine, 0.25%(w/v) Albumax II (Gibco), and gentamycin (50 ug/ml). The parasites were maintained at a hematocrit of 3% and were kept between 2% and 5% parasitemia or greater based on the needs of the individual experiments. Parasite synchronization was performed using 5% sorbitol (Lambros & Vandenberg, 1979).

To generate transgenic AP2-G2::GFP and AP2-G2 KO lines, transfections were carried out according to a standard protocol (Deitsch et al., 2001). The plasmid pDC2-cam-AP2-G2-GFP was transfected into the 3D7 strain of *P. falciparum* whereas pSLI-TGD-AP2-G2 was transfected into the 3D7 clone, E5 (Rovira-Graells et al., 2012). In brief, 100 μg of plasmid DNA (maxi prepped using Qiagen kit) was preloaded into O + RBCs at 50% hematocrit in cytomix prior to culturing with parasite-infected RBCs. After reinvasion, media containing 2.5 nM WR99210 was added to select for transgenic parasites. Stable integrants were maintained under constant drug pressure and were PCR-verified using specific primers (P1, P2, P4, P5, P6) outside the homology region after the isolation of gDNA (DNeasy Blood and Tissue kit, Qiagen). The resulting PfAP2G2::GFP and *pfap2-g2* KO parasites were cloned by limiting dilution (Rosario, 2008) and verified by diagnostic PCR (Figures S1 and 2a) and whole genome

sequencing. Sequencing analysis was done by creating a reference genome with GFP and rest of the plasmid at the expected location and reads were aligned to it.

4.3 | *Plasmodium falciparum* gametocyte production

Gametocytes were generated using the nutrient deprivation induction method as described (Miao et al., 2013). Briefly, synchronized trophozoites were cultured at ~2% parasitemia using 50% fresh RBC at 4% hematocrit. When the parasitemia reached 7%–10%, gametocyte production was induced by nutrient deprivation. The following day, stressed schizonts were split 50% into two flasks by adding fresh blood and fresh media. The following day, ring-stage committed gametocytes were counted as Day 1 of gametocytogenesis. To prevent the reinvasion and propagation of asexual parasites, parasites were treated with media with heparin (20 U/ml) from Day 1 post induction through Day 4. The media was changed daily to ensure the proper development and growth of the gametocytes.

4.4 | Nuclear and cytoplasmic protein extraction from parasites for western blotting

Nuclear and cytoplasmic extracts from parasites were prepared as previously described (Voss et al., 2002) using 5%–7% of the synchronized parasites. The proteins from the nuclear and cytoplasmic fractions were run on a gel (mini PROTEAN precast TGX gels) and then transferred to a nitrocellulose membrane. The membrane was then blocked using 5% w/v non-fat milk powder in 1X PBS-0.05% v/v Tween for 45 min at room temperature. The membrane was then incubated overnight at 4°C with an anti-GFP (ROCHE Anti-GFP, from mouse IgG1K, Millipore Sigma) (1:1,000), anti-histone (Anti-Histone H3 antibody, AbCam) (1:3,000), or anti-aldolase (Anti-Plasmodium aldolase antibody (HRP), AbCam) (1:1,000) primary antibody in the blocking buffer. After incubation, the membrane was washed three times with 1X PBS-0.05% v/v Tween and was incubated with the appropriate secondary antibodies, then washed. The secondary antibodies used were as follows: peroxidase-conjugated goat anti-rat HRP conjugate (Millipore) / goat anti-rabbit HRP conjugate (Millipore) / goat anti-mouse HRP conjugate (Pierce) was used (1:3,000). Bound antibodies were then visualized on a film after enhancing the signal with ECL (Pierce) as the substrate.

4.5 | Parasite growth assays and multiplication rate

To compare the growth rates of WT and *pfap2-g2* KO parasites we used a SYBR green growth assay (Vossen et al., 2010). Parasites were sampled every 24 hr for 10 days, starting at 0.1% parasitemia at the trophozoite stage. Both the WT and *pfap2-g2* KO strains were synchronized using 5% w/v sorbitol (described above) 3x before the start of the time course. Parasites were seeded in a 25 cm^2 culture flask at 0.1% parasitemia and 3% hematocrit. To evaluate growth differences every 24 hr for 10 days, 100 μl of parasite culture was collected in triplicate, transferred to a 96-well plate, and stored at −80°C. Following the completion of the time course, the parasites were thawed at room temperature, 100 μl of SYBR green I (Molecular Probes, Eugene Oregon) was diluted into parasite lysis buffer (20mM Tris–HCl pH 7.5, 5mM EDTA, 0.08% Triton X-100, 0.008% saponin in PBS) (0.2 μl of SYBR Green I/ml of lysis buffer) and added to each well and mixed. The plates were incubated at 37°C for 2 hr. Cell growth was measured as quantitation of DNA by SYBR green I using a Tecan GENios microplate detection device at the excitation wavelength and emission wavelength of 485 nm and 535 nm, respectively. All values were plotted as an average of three biological replicates (±S.D.) using GraphPad Prism (version 7). Linear model construction and ANOVA statistical analysis were performed in R (https://www.r-project.org). To calculate the multiplication rate, three independent biological experiments were performed in which synchronized WT and *pfap2-g2* KO parasites were seeded at 1% parasitemia and monitored for subsequent reinvasion of red blood cells. After reinvasion the number of ring stage parasites were counted from Giemsa-stained smears by microscopy.

4.6 | RNA purification and cDNA synthesis for DNA microarrays

Total RNA was extracted from tighSecttly synchronized PfAP2-G2::KO and WT parasites every 6 hr, starting at 3 hpi, throughout the 48 hr asexual life cycle. A separate time course was designed to collect RNA from gametocytes starting at Day 1 and every 12 hr for the following 7 days. RNA was extracted from parasite-infected RBCs collected at each time point using TRIzol (Thermo Fisher Scientific), following the manufacturer's protocol. cDNA synthesis and DNA microarray analysis was carried out as previously described (Painter et al., 2013). Two-channel Agilent DNA microarrays (AMADID 037,237) were hybridized, washed, and scanned on an Agilent G2600D Microarray SureScan Scanner. Signal intensities for each gene were extracted from the scanned image using Agilent Feature Extraction Software version 11.5.1.1. Detailed microarray protocols can be found at http://llinaslab.psu.edu/protocols/. The datasets were analyzed by Significance Analysis of Microarrays (SAM) (Tusher et al., 2001) for the significantly (>1.5 log2FC, 0.30 local FDR) changing genes between the WT and *ap2-g2* KO lines using two-class paired *t* test throughout each of the two time-courses. No data were available for the gametocyte TP6 due to technical reasons. All heat maps were clustered using Cluster 4.0 and was visualized using Java Tree View.

4.7 | Chromatin immunoprecipitation and Library preparation for sequencing (ChIP-Seq)

ChIP was performed as described (Josling et al., 2020) using synchronized trophozoite and gametocyte stage PfA2-G2-GFP parasites

(around 7% parasitemia). Extracted chromatin was sheared in SDS lysis buffer (10 mM HEPES pH 7.9, 10 mM KCl, 0.1 mM EDTA pH 8.0, 0.1 mM EGTA pH 8.0, 1 mM DTT and protease inhibitors) (200 μl 1x 10^9 trophozoites and 5x10^8 gametocytes) to obtain a fragment size of 100-150bp using an M220 focused-ultrasonicator (Covaris Inc.) using the following settings: peak power 75W, 2% duty factor, 200 cycles per burst and total treatment time of 600 s. Sonication time was optimized for PfAP2-G2 using the crosslinked DNA and shearing it for 0, 4, 8, 10, 12, and 15 min and then running it on agarose gel for the size estimate. For immunoprecipitations, sheared chromatin was pre-cleared using 20 μl/ml of magnetic beads A/G (Millipore 16–663) for 2 hr at 4°C with gentle agitation. The supernatant was collected and 50μl of the aliquot was removed as input. The rest of the chromatin was incubated overnight at 4°C with 1 μg of polyclonal anti-GFP antibody (Abcam ChIP grade, Abcam 290) or, as control, the same amount of IgG. The immunoprecipitated antibody/chromatin complex was collected using Protein A/G magnetic beads (Millipore 16–663). The input and ChIP samples were reverse cross-linked overnight at 45°C using 0.2M final concentration of NaCl. The samples were then treated with RNAase (30min at 37°C) and proteinase K (3 μl of 20 mg/ml with 2 hr incubation at 45°C) and purified using the QIAGEN MinElute PCR purification kit. Library was prepared as described earlier (Santos et al., 2017). The final library was quantified using a Qubit fluorometer HD DNA kit and analyzed using an Agilent DNA 1,000 Bioanalyzer to assess the quality, size distribution, and detection of any artifacts. Sequencing was performed using an Illumina Hiseq 2,500 to obtain 150 bp single-end reads.

4.8 | ChIP-seq data analysis

ChIP-seq data analysis was done using tools in Galaxy (usegalaxy.org). Before starting the analysis, the quality of the sequencing reads were assessed using FastQC and were trimmed to remove adapter and low quality bases using Trimmomatic (Bolger et al., 2014). The resulting reads were mapped to the *P. falciparum* genome (Pf 3D7 v28, obtained from PlasmoDB) using BWA-MEM (Li & Durbin, 2009) and duplicates reads were removed using SAMtools (Li et al., 2009). Mapped sequences were converted into bigwig files using bamCoverage (Ramírez et al., 2016) and were viewed in using the Integrative Genomics Viewer (IGV) (Thorvaldsdóttir et al., 2013) for each input and treatment. MACS2 (Feng et al., 2012) was used to call peaks with q-value cutoff of 0.05. The common overlapping intervals between replicates were established using Multiple Intersect function of BEDtools, and the overlapping intervals were combined into a single file using MergeBED (Quinlan & Hall, 2010). The genes closest to the peak summits were identified using closestBED. Peaks that were farther than 2.5 Kb were removed from the analysis. When the peak was present between two genes then only the gene closest to the peak was considered for the analysis.

Peak sequences were extracted using extract genomic DNA tool using genomic coordinates, and motifs associated with called peaks were identified using DREME (Bailey, 2011) and compared to identified ApiAP2 motifs using TOMTOM (Gupta et al., 2007). The correlation heatmap of the replicates performed on GFP tagged PfAP2-G2 ChIP-seq was made using multiBigwigSummary and plotCorrelation in the deepTools suite (Ramírez et al., 2016).

4.9 | Correlation analysis of PfAP2-G2 with other histone marks

Correlations were calculated between the occupancy of PfAP2-G2 and that of various histone marks previously reported in the literature, including H3K9me3, H4ac, H4K20me3, H3K26ac, H3K9ac, H3K4me3 (Karmodiya et al., 2015), H3K36me2 and H3K36me3 (Jiang et al., 2013) and heterochromatin protein 1 (Brancucci et al., 2014) First, read counts were obtained from PfAP2-G2 and nine histone marks in the gene body of all *P. falciparum* genes (n = 5,735; PlasmoDB annotations, release 28.0). NCIS (Liang & Keleş, 2012) was used to scale a control input experiment to each analyzed signal ChIP-seq experiment. Pairwise Pearson correlation coefficient of normalized read counts across 5,735 regions for PfAP2-G2 and nine histone marks. Then, proteins were ordered using complete-linkage hierarchical clustering with Euclidean distance.

4.10 | PfAP2-G2-GFP Immunoprecipitation and Mass Spectrometry

Nuclear extraction was performed from the PfAP2-G2::GFP parasites using lysis buffer (20 mM HEPES pH 7.8, 10 mM KCl, 1 mM EDTA, 1 mM DTT, 1x protease inhibitors) and a high salt extraction buffer (20 mM HEPES pH 7.8, 800 mM KCl, 1 mM EDTA, 1 mM DTT, 1x protease inhibitors) as previously described (Voss et al., 2002). A day before the immunoprecipitation, ~1mg of M-270 Epoxy Dynabeads (Invitrogen) per 100 ml of culture were conjugated with polyclonal anti-GFP antibodies at concentration of 5ug/mg (Abcam ab290) or with IgG (Abcam ab46540) overnight at 30°C as previously described (Joshi et al., 2013). Immunoprecipitation was carried out after washing the conjugated beads three times with dilution buffer (20 mM HEPES pH 7.8, 1 mM EDTA, 1 mM DTT, 1x protease inhibitors) and incubating with diluted nuclear extracts for 90 min at 4°C. The beads were again washed five times with dilution buffer and three times with cold 1X PBS. Protein was eluted using 20 μl loading buffer by shaking for 10 min at 70°C at 1,000 rpm and protein was stored at −20°C. Samples were quality controlled by western blotting and subjected to in-gel tryptic digest.

For tryptic digest the samples in polyacrylamide gel slices were destained with 50mM AmBic/50% ACN (Acetonitrile) and dehydrated using 100% ACN. Disulfide bonds in protein were reduced with 10mM DTT and reduced cysteine residues were then alkylated with 50mM iodoacetamide. Finally, the processed samples were digested with trypsin (Trypsin gold Promega, 6ng/μl) overnight at 37°C

on a thermomixer, and peptides were extracted from the gels. The dried peptide pellets were analyzed LC-MS/MS using a Q Exactive mass spectrometer (Indiana University Core Proteomics).

The data were processed using Trans-Proteomic Pipeline (TPP) as previously described with a few modifications (Deutsch et al., 2010). Spectra were searched against the *P. falciparum* proteome and contaminant repository database (CRAPome) using tandem and comet searches (Mellacheruvu et al., 2013). This search was combined in InterProphet and the proteins were searched with ProteinProphet. Only proteins with error rate less than 0.01 were reported. The immunopurification assay was performed time times and the data were combined to identify the significantly enriched proteins between the IP and control using SAINT (Choi et al., 2011). Proteins with probability score of 0.99 or greater were considered for analysis.

ACKNOWLEDGMENTS

This project was largely funded by NIH/NIAID 1R01 AI125565 (ML). NY and SM were supported by R01 GM121613 (SM) and JMS was supported by a Swiss National Fund GEP3-13613 and EMBO Long-Term Fellowship 633-2011. We thank Kelly Rios for assistance with proteomic data analysis and Scott Lindner for critical feedback.

DATA AVAILABILITY STATEMENT

All ChIP-seq sequencing reads are deposited at the NCBI Sequence Read Archive (SRA) in the Gene Expression Omnibus (GEO) under the accession number GSE157753. All DNA microarray data are also deposited at GEO under accession number GSE160923 (asexual) and GSE160924 (sexual gametocyte). Whole genome sequencing reads for *ap2-g2 gfp* and *ap2-g2* KO parasites are directly submitted to SRA under accession number PRJNA673876.

ORCID

Suprita Singh https://orcid.org/0000-0002-8271-7771
Joana M. Santos https://orcid.org/0000-0002-5411-4439
Lindsey M. Orchard https://orcid.org/0000-0003-1295-3733
Riëtte van Biljon https://orcid.org/0000-0002-1710-0441
Heather J. Painter https://orcid.org/0000-0003-0264-4689
Manuel Llinás https://orcid.org/0000-0002-6173-5882

REFERENCES

Aguilar, R., Magallon-Tejada, A., Achtman, A.H., Moraleda, C., Joice, R., Cisteró, P. et al (2014) Molecular evidence for the localization of *Plasmodium falciparum* immature gametocytes in bone marrow. *Blood*, *123*(7), 959–966. https://doi.org/10.1182/blood-2013-08-520767

Alano, P., Premawansa, S., Bruce, M.C. & Carter, R. (1991) A stage specific gene expressed at the onset of gametocytogenesis in *Plasmodium falciparum*. *Molecular and Biochemical Parasitology*, *46*(1), 81–88. https://doi.org/10.1016/0166-6851(91)90201-G

Armistead, J.S., Moraes, R.R., Barros, T.J., Gibson, W.A., Kite, J.P., Mershon, L.E. et al (2018) Infection of mosquitoes from in vitro cultivated plasmodium knowlesi H strain. *International Journal for Parasitology*, *48*(8), 601–610. https://doi.org/10.1016/j.ijpara.2018.02.004

Bailey, T.L. (2011) DREME: motif discovery in transcription factor ChIP-Seq data. *Bioinformatics*, *27*(12), 1653–1659. https://doi.org/10.1093/bioinformatics/btr261

Balaji, S., Madan Babu, M., Iyer, L.M. & Aravind, L. (2005) Discovery of the principal specific transcription factors of apicomplexa and their implication for the evolution of the AP2-integrase DNA binding domains. *Nucleic Acids Research*, *33*(13), 3994–4006. https://doi.org/10.1093/nar/gki709

Beeson, J.G., Drew, D.R., Boyle, M.J., Feng, G., Fowkes, F.J.I. & Richards, J.S. (2016) Merozoite surface proteins in red blood cell invasion, immunity and vaccines against malaria. *FEMS Microbiology Reviews*, *40*(3), 343–372. https://doi.org/10.1093/femsre/fuw001

Biljon, V., Riëtte, R.V., Wyk, H.J., Painter, L.O., Reader, J., Niemand, J. et al (2019) Hierarchical transcriptional control regulates *Plasmodium falciparum* sexual differentiation. *BMC Genomics*, *20*(1), 1–16.

Birnbaum, J., Flemming, S., Reichard, N., Soares, A.B., Mesén-Ramírez, P., Jonscher, E. et al (2017) A genetic system to study *Plasmodium falciparum* protein function. *Nature Methods*, *14*(4), 450–456. https://doi.org/10.1038/nmeth.4223

Bischoff, E. & Vaquero, C. (2010) In silico and biological survey of transcription-associated proteins implicated in the transcriptional machinery during the erythrocytic development of *Plasmodium falciparum*. *BMC Genomics*, *11*(1), 34. https://doi.org/10.1186/1471-2164-11-34

Bolger, A.M., Lohse, M. & Usadel, B. (2014) Trimmomatic: a flexible trimmer for illumina sequence data. *Bioinformatics*, *30*(15), 2114–2120. https://doi.org/10.1093/bioinformatics/btu170

Bozdech, Z., Llinás, M., Pulliam, B.L., Wong, E.D., Zhu, J. & DeRisi, J.L. (2003) The transcriptome of the intraerythrocytic developmental cycle of *Plasmodium falciparum*. *PLoS Biology*, *1*(1), 85–100. https://doi.org/10.1371/journal.pbio.0000005

Brancucci, N.M.B., Bertschi, N.L., Zhu, L., Niederwieser, I., Chin, W.H., Wampfler, R. et al (2014) Heterochromatin protein 1 secures survival and transmission of malaria parasites. *Cell Host and Microbe*, *16*(2), 165–176. https://doi.org/10.1016/j.chom.2014.07.004

Bruce, M.C., Alano, P., Duthie, S. & Carter, R. (1989) Commitment of the malaria parasite *Plasmodium falciparum* to sexual and asexual development. *Parasitology*, *100*(2), 191–200.

Bruce, M.C., Carter, R.N., Nakamura, K.-I., Aikawa, M. & Carter, R. (1994) Cellular location and temporal expression of the *Plasmodium falciparum* sexual stage antigen Pfs16. *Molecular and Biochemical Parasitology*, *65*(1), 11–22. https://doi.org/10.1016/0166-6851(94)90111-2

Bryant, J.M., Baumgarten, S., Dingli, F., Loew, D., Sinha, A., Claës, A. et al (2020) Exploring the virulence gene interactome with CRISPR/DC As9 in the human malaria parasite. *Molecular Systems Biology*, *16*(8), 1–22.

Campbell, T.L., de Silva, E.K., Olszewski, K.L., Elemento, O. & Llinás, M. (2010) Identification and genome-wide prediction of DNA binding specificities for the ApiAP2 family of regulators from the malaria parasite. *PLoS Path*, *6*(10), e1001165. https://doi.org/10.1371/journal.ppat.1001165

Chantalat, S., Depaux, A., Héry, P., Barral, S., Thuret, J.Y., Dimitrov, S. et al (2011) Histone H3 trimethylation at lysine 36 is associated with constitutive and facultative heterochromatin. *Genome Research*, *21*(9), 1426–1437. https://doi.org/10.1101/gr.118091.110

Chattopadhyay, R., Rathore, D., Fujioka, H., Kumar, S., De la Vega, P., Haynes, D. et al (2003) PfSPATR, a *Plasmodium falciparum* protein containing an altered thrombospondin type I Repeat domain is expressed at several stages of the parasite life cycle and is the target of inhibitory antibodies. *Journal of Biological Chemistry*, *278*(28), 25977–25981.

Choi, H., Larsen, B., Lin, Z.Y., Breitkreutz, A., Mellacheruvu, D., Fermin, D. et al (2011) SAINT: probabilistic scoring of affinity purificationg-mass spectrometry data. *Nature Methods*, *8*(1), 70–73.

Deitsch, K.W., Driskill, C.L. & Wellems, T.E. (2001) Transformation of malaria parasites by the spontaneous uptake and expression of DNA from human erythrocytes. *Nucleic Acids Research*, *29*(3), 850–853. https://doi.org/10.1093/nar/29.3.850

Deutsch, E.W., Mendoza, L., Shteynberg, D., Farrah, T., Lam, H., Tasman, N. et al (2010) A guided tour of the trans-proteomic pipeline. *Proteomics*, *10*(6), 1150–1159.

Duffy, P.E. & Kaslow, D.C. (1997) A novel malaria protein, Pfs28, and Pfs25 are genetically linked and synergistic as falciparum malaria transmission-blocking vaccines. *Infection and Immunity*, *65*(3), 1109–1113. https://doi.org/10.1128/IAI.65.3.1109-1113.1997

Ecker, A., Bushell, E.S.C., Tewari, R. & Sinden, R.E. (2008) Reverse genetics screen identifies six proteins important for malaria development in the mosquito. *Molecular Microbiology*, *70*(1), 209–220. https://doi.org/10.1111/j.1365-2958.2008.06407.x

Elemento, O., Slonim, N. & Tavazoie, S. (2007) A universal framework for regulatory element discovery across all genomes and data types. *Molecular Cell*, *28*(2), 337–350. https://doi.org/10.1016/j.molcel.2007.09.027

Espinosa, D.A., Vega-Rodriguez, J., Flores-Garcia, Y., Noe, A.R., Muñoz, C., Coleman, R. et al (2017) The *Plasmodium falciparum* cell-traversal protein for ookinetes and sporozoites as a candidate for preerythrocytic and transmission-blocking vaccines. *Infection and Immunity*, *85*(2), 1–10. https://doi.org/10.1128/IAI.00498-16

Farhat, D.C., Swale, C., Dard, C., Cannella, D., Ortet, P., Barakat, M. et al (2020) A MORC-driven transcriptional switch controls toxoplasma developmental trajectories and sexual commitment. *Nature Microbiology*, *5*(4), 570–583. https://doi.org/10.1038/s41564-020-0674-4

Feng, J., Liu, T., Qin, B.O., Zhang, Y. & Liu, X.S. (2012) Identifying ChIP-Seq enrichment using MACS. *Nature Protocols*, *7*(9), 1728–1740. https://doi.org/10.1038/nprot.2012.101

Fidock, D.A., Nomura, T., Talley, A.K., Cooper, R.A., Dzekunov, S.M., Ferdig, M.T. et al (2000) Mutations in the *P. falciparum* digestive vacuole transmembrane protein PfCRT and evidence for their role in chloroquine resistance. *Molecular Cell*, *6*(4), 861–871. https://doi.org/10.1016/S1097-2765(05)00077-8

Flueck, C., Bartfai, R., Niederwieser, I., Witmer, K., Alako, B.T.F., Moes, S. et al (2010) A Major Role for the *Plasmodium falciparum* ApiAP2 protein PfSIP2 in chromosome end biology. *PLoS Path*, *6*(2). https://doi.org/10.1371/journal.ppat.1000784

Flueck, C., Bartfai, R., Volz, J., Niederwieser, I., Salcedo-Amaya, A.M., Alako, B.T.F. et al (2009) *Plasmodium falciparum* heterochromatin protein 1 marks genomic loci linked to phenotypic variation of exported virulence factors. *PLoS Path*, *5*(9), e1000569. https://doi.org/10.1371/journal.ppat.1000569

Furuya, T., Mu, J., Hayton, K., Liu, A., Duan, J., Nkrumah, L. et al (2005) Disruption of a *Plasmodium falciparum* gene linked to male sexual development causes early arrest in gametocytogenesis. *Proceedings of the National Academy of Sciences*, *102*(46), 16813–16818.

Gautret P., Motard A. (1999) Periodic infectivity of Plasmodiumgametocytes to the vector. A review. *Parasite*, *6* (2), 103–111. https://doi.org/10.1051/parasite/1999062103

Gratraud, P., Huws, E., Falkard, B., Adjalley, S., Fidock, D.A., Berry, L. et al (2009) Oleic acid biosynthesis in *Plasmodium falciparum*: characterization of the stearoyl-CoA desaturase and investigation as a potential therapeutic target. *PLoS One*, *4*(9), e6889. https://doi.org/10.1371/journal.pone.0006889

Guizetti, J., Martins, R.M., Guadagnini, S., Claes, A. & Scherfa, A. (2013) Nuclear pores and perinuclear expression sites of var and ribosomal DNA genes correspond to physically distinct regions in *Plasmodium falciparum*. *Eukaryotic Cell*, *12*(5), 697–702.

Gupta, S., Stamatoyannopoulos, J.A., Bailey, T.L. & Noble, W.S. (2007) Quantifying similarity between motifs. *Genome Biology*, *8*(2), R24. https://doi.org/10.1186/gb-2007-8-2-r24

Heiss, K., Nie, H., Kumar, S., Daly, T.M., Bergman, L.W. & Matuschewski, K. (2008) Functional characterization of a redundant plasmodium TRAP family invasin, TRAP-like protein, by aldolase binding and a genetic complementation test. *Eukaryotic Cell*, *7*(6), 1062–1070. https://doi.org/10.1128/EC.00089-08

Ikadai, H., Saliba, K.S., Kanzok, S.M., McLean, K.J., Tanaka, T.Q., Cao, J. et al (2013) Transposon mutagenesis identifies genes essential for *Plasmodium falciparum* gametocytogenesis. *Proceedings of the National Academy of Sciences*, *110*(18), E1676–E1684.

Ishino, T., Yano, K., Chinzei, Y. & Yuda, M. (2004) Cell-Passage activity is required for the malarial parasite to cross the liver sinusoidal cell layer. *PLoS Biology*, *2*(1), 77–84. https://doi.org/10.1371/journal.pbio.0020004

Itsara, L.S., Zhou, Y., Do, J., Dungel, S., Fishbaugher, M.E., Betz, W.W. et al (2018) PfCap380 as a marker for *Plasmodium falciparum* oocyst development in vivo and in vitro. *Malaria Journal*, *17*(1), 1–13.

Jeninga, M., Quinn, J. & Petter, M. (2019) ApiAP2 Transcription factors in apicomplexan parasites. *Pathogens*, *8*(2), 47.

Jiang, L., Jianbing, M.U., Zhang, Q., Ni, T., Srinivasan, P., Rayavara, K. et al (2013) PfSETvs methylation of histone H3K36 represses virulence genes in *Plasmodium falciparum*. *Nature*, *499*(7457), 223–227.

Joice, R., Nilsson, S.K., Montgomery, J., Dankwa, S., Egan, E., Morahan, B. et al (2014) *Plasmodium falciparum* transmission stages accumulate in the human bone marrow. *Science Translational Medicine*, *6*(244), 1–9.

Joshi, P., Greco, T.M., Guise, A.J., Luo, Y., Fang, Y.U., Nesvizhskii, A.I. et al (2013) The functional interactome landscape of the human histone deacetylase family. *Molecular Systems Biology*, *9*(1), 1–21.

Josling, G.A., Russell, T.J., Venezia, J., Orchard, L., van Biljon, R., Painter, H.J. et al (2020) Dissecting the role of PfAP2-G in malaria gametocytogenesis. *Nature Communications*, *11*(1), 1503.

Josling, G.A., Williamson, K.C. & Llinás, M. (2018) Regulation of sexual commitment and gametocytogenesis in malaria parasites. *Annual Review of Microbiology*, *72*(1), 501–519.

Kafsack, B.F.C., Rovira-Graells, N., Clark, T.G., Bancells, C., Crowley, V.M., Campino, S.G. et al (2014) A transcriptional switch underlies commitment to sexual development in malaria parasites. *Nature*, *507*(7491), 248–252.

Karmodiya, K., Pradhan, S.J., Joshi, B., Jangid, R., Reddy, P.C. & Galande, S. (2015) A comprehensive epigenome map of *Plasmodium falciparum* reveals unique mechanisms of transcriptional regulation and identifies H3K36me2 as a global mark of gene suppression. *Epigenetics and Chromatin*, *8*(1), 1–18.

Kolasinska-Zwierz, P., Down, T., Latorre, I., Tao Liu, X., Liu, S. & Ahringer, J. (2009) Differential chromatin marking of introns and expressed exons by H3K36me3. *Nature Genetics*, *41*(3), 376–381.

Lambros, C. & Vandenberg, J.P. (1979) Synchronization of *Plasmodium falciparum* erythrocytic stages in culture. *Journal Parasitology*, *65*(3), 418–420. https://doi.org/10.2307/3280287

Li, H. & Durbin, R. (2009) Fast and accurate short read alignment with burrows-wheeler transform. *Bioinformatics*, *25*(14), 1754–1760. https://doi.org/10.1093/bioinformatics/btp324

Li, H., Handsaker, B., Wysoker, A., Fennell, T., Ruan, J., Homer, N. et al (2009) The sequence alignment/map format and SAMtools. *Bioinformatics*, *25*(16), 2078–2079. https://doi.org/10.1093/bioinformatics/btp352

Liang, K. & Keleş, S. (2012) Normalization of ChIP-Seq data with control. *BMC Bioinformatics*, *13*(1), 199. https://doi.org/10.1186/1471-2105-13-199

Lin, C.H., Paulson, A., Abmayr, S.M. & Workman, J.L. (2012) HP1a targets the drosophila KDM4A demethylase to a subset of heterochromatic genes to regulate H3K36me3 levels. *PLoS One*, *7*(6), e39758. https://doi.org/10.1371/journal.pone.0039758

Liu, Z., Miao, J. & Cui, L. (2011) Gametocytogenesis in malaria parasite: commitment, development and regulation. *Future Microbiology*, *6*(11), 1351–1369. https://doi.org/10.2217/fmb.11.108

Llorà-Batlle, O., Michel-Todó, L., Witmer, K., Toda, H., Fernández-Becerra, C., Baum, J. et al (2020) Conditional expression of PfAP2-G for controlled massive sexual conversion in *Plasmodium falciparum*. *Science Advances*, *6*(24), eaaz5057.

López-Barragán, M.J., Lemieux, J., Quiñones, M., Williamson, K.C., Molina-Cruz, A., Cui, K. et al (2011) Directional gene expression and antisense transcripts in sexual and asexual stages of *Plasmodium falciparum*. *BMC Genomics*, *12*. https://doi.org/10.1186/1471-2164-12-587

Mellacheruvu, D., Wright, Z., Couzens, A.L., Lambert, J.P., St-Denis, N.A., Li, T. et al (2013) The CRAPome: a contaminant repository for affinity purification-mass spectrometry data. *Nature Methods*, *10*(8), 730–736. https://doi.org/10.1038/nmeth.2557

Miao, J., Wang, Z., Liu, M., Parker, D., Li, X., Chen, X. et al (2013) *Plasmodium falciparum*: generation of pure gametocyte culture by heparin treatment. *Experimental Parasitology*, *135*(3), 541–545. https://doi.org/10.1016/j.exppara.2013.09.010

Miller, S.K., Good, R.T., Drew, D.R., Delorenzi, M., Sanders, P.R., Hodder, A.N. et al (2002) A subset of *Plasmodium falciparum* SERA genes are expressed and appear to play an important role in the erythrocytic cycle. *Journal of Biological Chemistry*, *277*(49), 47524–47532.

Modrzynska, K., Pfander, C., Chappell, L., Yu, L.U., Suarez, C., Dundas, K. et al (2017) A knockout screen of ApiAP2 genes reveals networks of interacting transcriptional regulators controlling the plasmodium life cycle. *Cell Host and Microbe*, *21*(1), 11–22. https://doi.org/10.1016/j.chom.2016.12.003

Mwakalinga S.B., Wang C.W., Bengtsson D.C., Turner L., Dinko B., Lusingu J.P., et al. (2012) Expression of a type B RIFIN in Plasmodium falciparum merozoites and gametes. *Malaria Journal*, *11* (1), 429. http://doi.org/10.1186/1475-2875-11-429

Neveu G., Dupuy F., Ladli M., Barbieri D., Naissant B., Richard C., et al. (2018) Plasmodium falciparum gametocyte-infected erythrocytes do not adhere to human primary erythroblasts. *Scientific Reports*, *8* (1), 1–11.

Neveu, G. & Lavazec, C. (2019) Erythrocyte membrane makeover by *Plasmodium falciparum* gametocytes. *Frontiers in Microbiology*, *10*(November), 1–8. https://doi.org/10.3389/fmicb.2019.02652

Nixon, C.P., Nixon, C.E., Michelow, I.C., Silva-Viera, R.A., Colantuono, B., Obeidallah, A.S. et al (2018) Antibodies to PfsEGXP, an early gametocyte-enriched phosphoprotein, predict decreased *Plasmodium falciparum* gametocyte density in humans. *Journal of Infectious Diseases*, *218*(11), 1792–1801. https://doi.org/10.1093/infdis/jiy416

Nunes, M.C., Dea, J.P., Goldring, C.D. & Scherf, A. (2007) A novel protein kinase family in *Plasmodium falciparum* Is differentially transcribed and secreted to various cellular compartments of the host cell. *Molecular Microbiology*, *63*(2), 391–403.

Oehring, S.C., Woodcroft, B.J., Moes, S., Wetzel, J., Dietz, O., Pulfer, A. et al (2012) Organellar proteomics reveals hundreds of novel nuclear proteins in the malaria parasite *Plasmodium falciparum*. *Genome Biology*, *13*(11), R108.

Painter, H.J., Altenhofen, L.M., Kafsack, B.F.C. & Llinás, M. (2013) Whole-genome analysis of Plasmodium Spp. utilizing a new agilent technologies DNA microarray platform. *Methods in Molecular Biology*, *923*, 213–219.

Painter, H.J., Campbell, T.L. & Llinás, M. (2011) The apicomplexan AP2 family: integral factors regulating plasmodium development. *Molecular and Biochemical Parasitology*, *176*(1), 1–7. https://doi.org/10.1016/j.molbiopara.2010.11.014

Painter, H.J., Carrasquilla, M. & Llinás, M. (2017) Capturing in vivo RNA transcriptional dynamics from the malaria parasite *Plasmodium falciparum*. *Genome Research*, *27*(6), 1074–1086.

Painter, H.J., Chung, N.C., Sebastian, A., Albert, I., Storey, J.D. & Llinás, M. (2018) Genome-wide real-time in vivo transcriptional dynamics during *Plasmodium falciparum* blood-stage development. *Nature Communications*, *9*(1), 1–12. https://doi.org/10.1038/s41467-018-04966-3

Pei, X., An, X., Guo, X., Tarnawski, M., Coppel, R. & Mohandas, N. (2005) Structural and functional studies of interaction between *Plasmodium falciparum* knob-associated Histidine-Rich protein (KAHRP) and erythrocyte spectrin. *Journal of Biological Chemistry*, *280*(35), 31166–31171.

Petter, M., Bonow, I. & Klinkert, M.Q. (2008) Diverse expression patterns of subgroups of the rif Multigene family during *Plasmodium falciparum* gametocytogenesis. *PLoS One*, *3*(11), e3779. https://doi.org/10.1371/journal.pone.0003779

Poran, A., Nötzel, C., Aly, O., Mencia-Trinchant, N., Harris, C.T., Guzman, M.L. et al (2017) Single-cell RNA sequencing reveals a signature of sexual commitment in malaria parasites. *Nature*, *551*(7678), 95–99. https://doi.org/10.1038/nature24280

Portugaliza, H.P., Miyazaki, S., Geurten, F.J.A., Pell, C., Rosanas-Urgell, A., Janse, C.J. et al (2020) Artemisinin exposure at the ring or trophozoite stage impacts *Plasmodium falciparum* sexual conversion differently. *Elife*, *9*, 1–22. https://doi.org/10.7554/eLife.60058

Quinlan, A.R. & Hall, I.M. (2010) BEDTools: a flexible suite of utilities for comparing genomic features. *Bioinformatics*, *26*(6), 841–842. https://doi.org/10.1093/bioinformatics/btq033

Rabinovich, R.N., Drakeley, C., Djimde, A.A., Fenton Hall, B., Hay, S.I., Hemingway, J. et al (2017) MalERA: an updated research agenda for malaria elimination and eradication. *PLoS Med*, *14*(11), 1–17. https://doi.org/10.1371/journal.pmed.1002456

Ramírez, F., Ryan, D.P., Grüning, B., Bhardwaj, V., Kilpert, F., Richter, A.S. et al (2016) DeepTools2: a next generation web server for deep-sequencing data analysis. *Nucleic Acids Research*, *44*(W1), W160–W165. https://doi.org/10.1093/nar/gkw257

Rawlings, D.J., Fujioka, H., Fried, M., Keister, D.B., Aikawa, M. & Kaslow, D.C. (1992) α-Tubulin II is a male-specific protein in *Plasmodium falciparum*. *Molecular and Biochemical Parasitology*, *56*(2), 239–250. https://doi.org/10.1016/0166-6851(92)90173-H

Rea, E., Le Roch, K.G. & Tewari, R. (2018) Sex in *Plasmodium falciparum*: silence play between GDV1 and HP1. *Trends in Parasitology*, *34*(6), 450–452. https://doi.org/10.1016/j.pt.2018.04.006

Rosario, V. (2008) Cloning of naturally occurring mixed infections of malaria parasites. *Advancement of Science*, *212*(4498), 1037–1038. https://doi.org/10.1126/science.7015505

Rovira-Graells, N., Gupta, A.P., Planet, E., Crowley, V.M., Mok, S., Pouplana, L.R.D. et al (2012) Transcriptional variation in the malaria parasite *Plasmodium falciparum*. *Genome Research*, *22*(5), 925–938. https://doi.org/10.1101/gr.129692.111

Santos, J.M., Josling, G., Ross, P., Joshi, P., Orchard, L., Campbell, T. et al (2017) Red blood cell invasion by the malaria parasite is coordinated by the PfAP2-I transcription factor. *Cell Host and Microbe*, *21*(6), 731–741.e10. https://doi.org/10.1016/j.chom.2017.05.006

Sargeant, T.J., Marti, M., Caler, E., Carlton, J.M., Simpson, K., Speed, T.P. et al (2006) Lineage-specific expansion of proteins exported to erythrocytes in malaria parasites. *Genome Biology*, *7*(2), R12.

Sharp S., Lavstsen T., Fivelman Q.L., Saeed M., McRobert L., Templeton T.J., et al. (2006) Programmed Transcription of the var Gene Family, but Not of stevor, in Plasmodium falciparum Gametocytes. *Eukaryotic Cell*, *5* (8), 1206–1214.

Silvestrini, F., Lasonder, E., Olivieri, A., Camarda, G., Van Schaijk, B., Sanchez, M. et al (2010) Protein export marks the early phase of gametocytogenesis of the human malaria parasite *Plasmodium falciparum*. *Molecular and Cellular Proteomics*, *9*(7), 1437–1448.

Sinden, R.E. (1982) Gametocytogenesis of *Plasmodium falciparum* in vitro: an electron microscopic study. *Parasitology*, *84*(1), 1–11.

Singh, A.P., Buscaglia, C.A., Wang, Q., Levay, A., Nussenzweig, D.R., Walker, J.R. et al (2007) Plasmodium circumsporozoite protein promotes the development of the liver stages of the parasite. *Cell*, *131*(3), 492–504. https://doi.org/10.1016/j.cell.2007.09.013

Sinha, A., Hughes, K.R., Modrzynska, K.K., Otto, T.D., Pfander, C., Dickens, N.J. et al (2014) A cascade of DNA-binding proteins for sexual commitment and development in plasmodium. *Nature*, *507*(7491), 253–257. https://doi.org/10.1038/nature12970

Thompson, J., Fernandez-Reyes, D., Sharling, L., Moore, S.G., Eling, W.M., Kyes, S.A. et al (2007) Plasmodium cysteine repeat modular proteins 1–4: complex proteins with roles throughout the malaria parasite life cycle. *Cellular Microbiology*, *9*(6), 1466–1480. https://doi.org/10.1111/j.1462-5822.2006.00885.x

Thorvaldsdóttir, H., Robinson, J.T. & Mesirov, J.P. (2013) Integrative genomics viewer (IGV): high-performance genomics data visualization and exploration. *Briefings in Bioinformatics*, *14*(2), 178–192. https://doi.org/10.1093/bib/bbs017

Tibúrcio, M., Niang, M., Deplaine, G., Perrot, S., Bischoff, E., Ndour, P.A. et al (2012) A switch in infected erythrocyte deformability at the maturation and blood circulation of *Plasmodium falciparum* transmission stages. *Blood*, *119*(24), 172–180. https://doi.org/10.1182/blood-2012-03-414557

Tibúrcio, M., Silvestrini, F., Bertuccini, L., Sander, A.F., Turner, L., Lavstsen, T. et al (2013) Early gametocytes of the malaria parasite *Plasmodium falciparum* specifically remodel the adhesive properties of infected erythrocyte surface. *Cellular Microbiology*, *15*(4), 647–659.

Toro-Moreno, M., Sylvester, K., Srivastava, T., Posfai, D. & Derbyshire, E.R. (2020) RNA-Seq analysis illuminates the early stages of plasmodium liver infection. *MBio*, *11*(1), e03234-19.

Trager W, Jensen J. (1976) Human malaria parasites in continuous culture. *Science*, *193*, 673–675. https://doi.org/10.1126/science.781840

Tusher, V.G., Tibshirani, R. & Chu, G. (2001) Significance analysis of microarrays applied to the ionizing radiation response. *Proceedings of the National Academy of Sciences of the United States of America*, *98*(9), 5116–5121. https://doi.org/10.1073/pnas.091062498

van Dijk, M.R., van Schaijk, B.C.L., Khan, S.M., van Dooren, M.W., Ramesar, J., Kaczanowski, S. et al (2010) Three members of the 6-Cys protein family of plasmodium play a role in gamete fertility. *PLoS Path*, *6*(4), 1–13.

Venugopal, K., Hentzschel, F., Valkiūnas, G. & Marti, M. (2020) Plasmodium asexual growth and sexual development in the haematopoietic niche of the host. *Nature Reviews Microbiology*, *18*(3), 177–189. https://doi.org/10.1038/s41579-019-0306-2

Villard, V., Agak, G.W., Frank, G., Jafarshad, A., Servis, C., Nébié, I. et al (2007) Rapid identification of malaria vaccine candidates based on α-helical coiled coil protein motif. *PLoS One*, *2*(7), e645.

Volz, J.C., Yap, A., Sisquella, X., Thompson, J.K., Lim, N.T.Y., Whitehead, L.W. et al (2016) Essential role of the PfRh5/PfRipr/CyRPA complex during *Plasmodium falciparum* invasion of erythrocytes. *Cell Host and Microbe*, *20*(1), 60–71. https://doi.org/10.1016/j.chom.2016.06.004

Voss, T.S., Mini, T., Jenoe, P. & Beck, H.P. (2002) *Plasmodium falciparum* possesses a cell cycle-regulated short type replication protein a large subunit encoded by an unusual transcript. *Journal of Biological Chemistry*, *277*(20), 17493–17501.

Vossen, M.G., Pferschy, S., Chiba, P. & Noedl, H. (2010) The SYBR Green I malaria drug sensitivity assay: performance in low parasitemia samples. *American Journal of Tropical Medicine and Hygiene*, *82*(3), 398–401. https://doi.org/10.4269/ajtmh.2010.09-0417

Weiss, D.J., Lucas, T.C.D., Nguyen, M., Nandi, A.K., Bisanzio, D., Battle, K.E. et al (2019) Mapping the global prevalence, incidence, and mortality of *Plasmodium falciparum*, 2000–17: a spatial and temporal modelling study. *The Lancet*, *394*(10195), 322–331. https://doi.org/10.1016/S0140-6736(19)31097-9

WHO. (2019) *World Malaria Report*.

Young, J.A., Fivelman, Q.L., Blair, P.L., De La Vega, P., Le Roch, K.G., Zhou, Y. et al (2005) The *Plasmodium falciparum* sexual development transcriptome: a microarray analysis using ontology-based pattern identification. *Molecular and Biochemical Parasitology*, *143*(1), 67–79. https://doi.org/10.1016/j.molbiopara.2005.05.007

Yuda, M., Iwanaga, S., Kaneko, I. & Kato, T. (2015). Global transcriptional repression: an initial and essential step for plasmodium sexual development. *Proceedings of the National Academy of Sciences of the United States of America 112*, 12824–12829.

Yuda, M., Kaneko, I., Iwanaga, S., Murata, Y. & Kato, T. (2019) Female-specific gene regulation in malaria parasites by an AP2-family transcription factor. *Molecular Microbiology*, *113*(1), 40–51. https://doi.org/10.1111/mmi.14334

Zhang, C., Li, Z., Cui, H., Jiang, Y., Yang, Z. & Wang, X.U. (2017) Systematic CRISPR-Cas9-mediated ApiAP2 genes reveal functional insights into parasite development. *MBio*, *8*(6), 1–17.

Zhang, M., Wang, C., Otto, T.D., Oberstaller, J., Liao, X., Adapa, S.R. et al (2018). Uncovering the essential genes of the human malaria parasite *Plasmodium falciparum* by saturation mutagenesis. *Science*, *360*(6388), eaap7847.

Zhao, J., Bhanot, P., Junjie, H.U. & Wang, Q. (2016) A Comprehensive analysis of plasmodium circumsporozoite protein binding to hepatocytes. *PLoS One*, *11*(8), 1–13. https://doi.org/10.1371/journal.pone.0161607

SUPPORTING INFORMATION

Additional Supporting Information may be found online in the Supporting Information section.

How to cite this article: Singh S, Santos JM, Orchard LM, et al. The PfAP2-G2 transcription factor is a critical regulator of gametocyte maturation. *Mol Microbiol*. 2021;00:1–20. https://doi.org/10.1111/mmi.14676